

Tightening Curves on Surfaces Monotonically with Applications

Hsien-Chih Chang* Arnaud de Mesmay†

February 5, 2020

Abstract

We prove the first polynomial bound on the number of *monotonic* homotopy moves required to tighten a collection of closed curves on any compact orientable surface, where the number of crossings in the curve is not allowed to increase at any time during the process. The best known upper bound before was exponential, which can be obtained by combining the algorithm of de Graaf and Schrijver [*J. Comb. Theory Ser. B*, 1997] together with an exponential upper bound on the number of possible surface maps. To obtain the new upper bound we apply tools from hyperbolic geometry, as well as operations in graph drawing algorithms—the cluster and pipe expansions—to the study of curves on surfaces.

As corollaries, we present two efficient algorithms for curves and graphs on surfaces. First, we provide a polynomial-time algorithm to convert any given multicurve on a surface into minimal position. Such an algorithm only existed for single closed curves, and it is known that previous techniques do not generalize to the multicurve case. Second, we provide a polynomial-time algorithm to reduce any k -terminal plane graph (and more generally, surface graph) using degree-1 reductions, series-parallel reductions, and ΔY -transformations for arbitrary integer k . Previous algorithms only existed in the planar setting when $k \leq 4$, and all of them rely on extensive case-by-case analysis based on different values of k . Our algorithm makes use of the connection between electrical transformations and homotopy moves, and thus solves the problem in a unified fashion.

*Department of Computer Science, Duke University, USA. Work by this author was partially supported by NSF under grants CCF-14-08763, CCF-15-13816, CCF-15-46392, and IIS-14-08846, by an ARO grant W911NF-15-1-0408, and by BSF Grant 2012/229 from the U.S.-Israel Binational Science Foundation.

†Université Paris-Est, LIGM, CNRS, ENPC, ESIEE Paris, UPEM, Marne-la-Vallée, France. Work by this author was partially supported by the French ANR projects ANR-18-CE40-0004-01 (FOCAL), ANR-17-CE40-0033 (SoS), ANR-16-CE40-0009-01 (GATO) and ANR-19-CE40-0014 (MINMAX).

1 Introduction

Let Σ be an arbitrary compact orientable surface, possibly with boundary. We consider a collection of closed curves (referred to as a *multicurve*) on Σ drawn in general position—with finitely many double crossings, each of which is a transverse intersection, and no tangents or crossings of higher orders. The goal is to *tighten* the closed curves into another collection of curves with a minimum number of crossings using only continuous deformations known as *homotopy*. The minimum number of crossings achievable under homotopy is known as the *geometric intersection number*, a fundamental topological parameter associated with any set of closed curves on a surface. There are many previous works, both in theory and in practice, describing how to compute the geometric intersection number and the tightening process more or less efficiently; we refer to the extensive historical notes of Despré and Lazarus [22] for more background on this classical problem.

Different papers measured the efficiency of the algorithms in different ways; in this paper we are in particular interested in minimizing the total number of combinatorial changes to the closed curves. Using standard arguments [4, 5, 54], every homotopy can be decomposed into a finite sequence of local changes called the *homotopy moves*, consisting of the following three basic operations: undo a monogon, remove a bigon, and flip a triangle. See Figure 1.1 for an illustration.



Figure 1.1. The three homotopy moves 1→0, 2→0, and 3→3.

Here our goal is to provide an upper bound on the number of homotopy moves used to tighten a given collection of curves. Furthermore, a desired property of the tightening process is that at no times the number of crossings increases throughout the homotopy. Intuitively this is a natural property to assume; after all, the goal is to minimize the final number of crossings, and in a sense we want to perform the algorithm greedily and never make the curves more complicated. In addition, as we will explain later on, monotonicity is not merely a natural assumption to enforce on the tightening process, it is also the key property to draw connection to other sets of local transformations. Surprisingly, proving that such a monotonic tightening process exists actually requires quite involved arguments, and it was only shown by Hass and Scott [41] and de Graaf and Schrijver [38] that we can safely make such an assumption. Both algorithms used some discrete variants of the curve-shortening technique of Grayson [39], Shepard [58], and Angenent [6]. The main downside of the approach is that these algorithms are not *efficient* when measured in combinatorial changes. Indeed, none of the authors of previous algorithms analyze their performance, and with careful reading the best upper bound on the number of homotopy moves performed is merely exponential. Ideally, we would like to have the best of two worlds—a tightening process that is efficient while never creating new crossings.

1.1 Our results

In this paper we prove that any collection of closed curves on an orientable surface (possibly with boundary) of genus $g \geq 2$ can be tightened using a polynomial number of monotonic homotopy moves.

Theorem 1.1. *Any n -vertex multicurve γ on an orientable surface Σ of genus g with $b > 0$ boundary components can be tightened monotonically using $O((g + b)n^3)$ homotopy moves. When the surface Σ does not have any boundary component (that is, $b = 0$) and not a torus, the upper bound becomes $O(n^5 \log^3 g / g^2 + gn^3)$.*

Note that our theorem applies to surface with any combination of genus and number of boundary components with the one exception of a boundaryless torus. The result improves over the previous monotonic reduction algorithm by de Graaf and Schrijver [38] which, combined with the exponential bound on the number of surface maps [9] yielded an exponential upper bound. A recent article by Chang *et al.* [13] gave a polynomial upper bound on the number of homotopy moves. However, their algorithm does not guarantee monotonicity, and it only works for a *single* closed curve; in fact, it is understood that a completely new approach is required to overcome these shortcomings. Their algorithm relies on the *bigon removal approach* powered by the result of Hass and Scott [40], proving the existence of a *singular bigon* or *monogon*—that is, a bigon or monogon that overlaps itself in a not-too-pathological way. Such bigons and monogons can be removed using polynomially many homotopy moves (see for example [13, §4.2] and [10, §6.2.1]). However, it is known (see for example Figure 0.1 of Hass and Scott [40] or Figure 1 of Despré and Lazarus [22]) that such singular bigons may not exist when leaving the realm of single closed curves. Furthermore, every known algorithm that removes singular bigons increases the number of crossings temporarily during the homotopy process, and therefore is not monotonic.

The first application of our main theorem is that one can convert any given collection of closed curves into minimal position (that is, with a minimum number of crossings) using homotopy *in polynomial time*.

Theorem 1.2. *Given a multicurve γ on an orientable surface Σ , we can compute a minimal position of γ on Σ in polynomial time.*

As a corollary, we can compute in polynomial time the geometric intersection number of a multicurve, a problem for which the first polynomial-time algorithm was only provided very recently by Despré and Lazarus [22]. In that paper, Despré and Lazarus also provide a different algorithm to compute minimal position of a *single* closed curve in polynomial time. Since their techniques also rely on finding and removing singular bigons and monogons, it suffers from the same limitations as explained above and cannot be readily generalized to the more general setting of multicurves. The existence of an efficient algorithm is not immediate even assuming our main theorem; one has to carefully examine each step of the proof and make sure they can be implemented efficiently. While Theorem 1.1 does not apply to the case where Σ is a torus, we provide a separate algorithm to handle it.

The second application to the main theorem is the first polynomial-time algorithm that reduces any k -terminal plane graph (and more generally, any k -terminal surface graph) using *electrical transformations*—a collection of operations on surface graphs consists of degree-1 reductions, series-parallel reductions, and ΔY -transformations. It is required that all transformations respect the embedding of the graph, and no terminals can be removed during the reduction. The goal is to perform a sequence of electrical transformations on the input surface graph and reduce the graph as much as possible—that is, to obtain another surface graph that minimizes the number of edges.

Theorem 1.3. *Any surface graph with terminals can be reduced as much as possible using electrical transformations in polynomial time.*

Electrical transformations have been widely applied to graph algorithms and network optimizations [1, 28, 37, 45, 47] and other fields of science and engineering [16, 44, 49, 53, 59, 67]. For a history of electrical transformations and other related work, see [10]. The relation between electrical transformations and homotopy has been studied implicitly since Tait [63], Steinitz [60, 61], and Yajima and Kinoshita [66], and explicitly by Goldman and Kauffman [35] and Nobel and Welsh [51], through the lens of *medial construction*. The *medial graph* G^\times of a surface embedded graph G is constructed as follows: create a vertex for each edge in G , and create an edge between two vertices if the corresponding two edges share

both a vertex and a face in G . From the construction it is immediate that every vertex in G^\times has degree 4. So one can decompose the medial graph into a collection of curves γ by making each vertex of G^\times an intersection point between two constituent curves of γ . Quantitative connection between the two sets of operations has been established first in the plane [12], and later for general surfaces [10, 11]. The most important observation we rely on is the following: Any polynomial upper bound on the number of monotonic homotopy moves required to tighten the medial multicurve G^\times turns into a polynomial upper bound on the number of electrical transformations required to reduce the surface graph G . Furthermore, the same statement holds when one replaces “number of moves” with “running time”.

There are polynomial-time algorithms that reduce any surface graph with 2-terminals [29, 65], 3-terminals [33, 34, 52], and 4-terminals [7, 21]. As for arbitrary value of k , previous algorithms assume special positions of the terminals, say when all terminals lie on a single face of the plane graph [18, 33]. All these algorithms, especially the ones for constant number of terminals, rely on heavy case-by-case analysis to characterize what the reduced graphs look like (for example, the work of Archdeacon *et al.* [7] and Demasi and Mohar [21] for the 4-terminal case in total span more than a hundred pages). In contrast, our algorithm functions in a unified way by transforming the graph reduction problem into a curve tightening problem on a surface using a set of local operations similar to homotopy moves (see Section 5.2), and therefore avoids the above complications. The electrical reduction algorithm relies crucially on the fact that the curve tightening process is efficient, monotone, and works for multicurves; this is why previous results [13, 22, 38] cannot be used. An important subtlety is that the aforementioned algorithms to reduce surface graphs with terminals also allow the use of one additional move called the *terminal-leaf contraction*. We explain in Section 5.3 how this additional move can also be integrated within our framework.

Our efficient electrical reduction algorithm is the conclusion of a long sequence of works [10, 11, 12, 13] and our main philosophical contribution—curves and graphs on surfaces can be reduced efficiently when measured in combinatorial changes.

1.2 Technical contribution

The proof of Theorem 1.1 can be viewed as an amalgamation of the curve shortening algorithm of de Graaf and Schrijver [38], the cluster and pipe expansion technique from graph drawings [15, 19, 30], and the crossing minimization algorithm for flat braids originated from Geck and Pfeiffer in the context of word problem over symmetric groups [32, 38]. The first step relies on hyperbolic geometry, which is very relevant to our tightening problem for the following reasons: (1) any (multi)curve on a surface endowed with a hyperbolic metric is homotopic to a unique (multi)geodesic, and (2) a primitive (multi)geodesic is in minimal position. Our proof follows this approach closely but the key challenge is to control the combinatorics of the curves as well as the length of the process.

Therefore, our first step is to endow Σ with a hyperbolic metric, and to move the multicurve γ to a neighborhood of the unique collection of geodesics of its homotopy class. Unlike de Graaf and Schrijver [38], we cannot afford to move the multicurve all the way until it reaches a canonical braid-like form. Instead, we execute the curve shortening algorithm frugally until the curves lie in the ε -neighborhoods of its geodesics, where ε is chosen just small enough to ensure that these neighborhoods do not cover the entire surface. Since we know that the curves can be tightened further while staying in the neighborhoods, at this point it is safe to put a puncture on the uncovered surface and reduce the problem to curves on (orientable) surfaces with boundary.

The second step relies on the new observation that, for a collection of curves γ on surface with boundary, one can perform a quadratic number of homotopy moves and put the curves into a *pipe system*—a regular neighborhood of some one-dimensional skeleton graph. Then multicurve γ along with the pipe system are modified gradually by the *expansion operations*, in a way that after polynomial many

steps, each constituent curve of γ is combinatorially close to a power of some primitive curve, which then can be turned into a canonical form that looks like a flat braid. After reaching the braid form we use the crossing minimization algorithm [32, 38] to make γ tight.

We summarize the above steps in the following two lemmas. Let γ be a collection of curves on a surface Σ of negative Euler characteristic, and let γ_* be the unique (multi)geodesic of γ on Σ . We say the multicurve γ is ε -close to the geodesic γ_* if the lift of γ in the universal cover lies in an ε -neighborhood of the lift of γ_* .

Lemma 1.4. *Let γ be an n -vertex non-contractible multicurve on a surface Σ of genus $g \geq 2$ without boundary, and let γ_* be the unique geodesic of γ on Σ . One can endow Σ with a hyperbolic metric so that the multicurve γ can be made ε -close to γ_* using $O(n^5 \log^3 g / g^2)$ monotonic homotopy moves for some $\varepsilon = \Theta(g / (n \log g))$; furthermore, the ε -neighborhood of γ_* does not cover the whole surface Σ .*

Lemma 1.5. *Let γ be an n -vertex multicurve with no contractible components on an orientable surface Σ of genus g with $b > 0$ boundary components. Then γ can be tightened using $O((g + b)n^3)$ monotonic homotopy moves.*

Theorem 1.1 follows rather directly from Lemma 1.4 and Lemma 1.5; this is explained in Section 2.4. We prove Lemma 1.4 in Section 3, and Lemma 1.5 in Section 4. Applications are discussed in Section 5.

2 Preliminaries

Familiarity with basic concepts regarding the topology and geometry of surfaces will greatly ease the reading. We recommend Stillwell [62] for a general combinatorial introduction to the topic, and the first chapter of Farb and Margalit [27] for the specific topic on curves, surfaces, and hyperbolic geometry.

2.1 Curves on surfaces

A *surface* Σ is a two-dimensional (topological) manifold, possibly with boundaries. All the surfaces in this article are compact, connected, and orientable. The *Euler characteristic* of a surface Σ is $2 - 2g - b$, where g is the genus and b the number of boundary components in Σ . A *closed curve* on a surface Σ is a continuous map $\gamma: S^1 \rightarrow \Sigma$. A *multicurve* is a collection of closed curves, which form its *constituent curves*. An *arc* or *path* on a surface Σ is a continuous map $\gamma: [0, 1] \rightarrow \Sigma$ with endpoints on the boundary. In general, we refer to either a collection of closed curve or arcs as *curves*. We only consider generic curves, that is, curves with only a finite number of self-intersections which are transverse double points. A *subpath* of a curve γ is the restriction of γ to an interval. A curve is *simple* if it is injective. We will consider sometimes closed curves as graphs embedded on Σ by treating their self-intersection points as vertices and the maximal subpaths between these vertices as edges. A *tangle* is a collection of boundary-to-boundary paths $\gamma_1, \dots, \gamma_s$ in a closed topological disk, which (self-)intersect only pairwise, transversely, and away from the boundary. We call each individual path a *strand* of the tangle.

A *homotopy* between two closed curves γ_1 and γ_2 is a continuous deformation $h: S^1 \times [0, 1] \rightarrow \Sigma$ such that $h(\cdot, 0) = \gamma_1$ and $h(\cdot, 1) = \gamma_2$. This definition extends naturally to arcs and multicurves. A closed curve is *contractible* if it is homotopic to a point. In this article, we take the convention that if at some point in a homotopy, a multicurve contains a contractible closed curve which has degenerated to a point, we can *remove* this contractible closed curve from the multicurve.¹ As explained in the introduction, classical arguments show that any homotopy between two closed curves in general position

¹Notice that this differs from de Graaf and Schrijver [38], which is why they require one more homotopy move than we do.

189 can be decomposed into a sequence of the three homotopy moves pictured in Figure 1.1. A multicurve is
 190 **tightened**, or **tight**, or is a **tightening**, or is in **minimal position** if it has the smallest possible number
 191 of intersections among all the multicurves within its homotopy class. Sometimes, it will be useful to
 192 specify in which surface a homotopy or a tightening lies, for example for a multicurve γ contained in a
 193 surface Σ which is a sub-surface of another surface Σ' ; in this case, we will talk about a homotopy, or a
 194 tightening, *within* Σ .

195 A **monogon**² for a curve γ is a subpath that begins and ends at the same vertex x and bounds a disk
 196 incident to only that vertex. A **bigon**² for a curve γ consists of two simple interior-disjoint subpaths
 197 of γ , sharing two endpoints that together bound a disk on Σ incident to only these two endpoints.
 198 Similarly, a **trigon**² for γ consists of three simple interior-disjoint subpaths of γ , forming three pairwise
 199 intersections that together bound a disk on Σ . A monogon, bigon, or trigon is **empty** when the interior
 200 of the bounded disk is disjoint from γ . A bigon is **minimal** or **innermost** if the disk it bounds does
 201 not contain a smaller bigon or monogon; a *minimal monogon* is defined similarly. Note that a minimal
 202 monogon does not contain anything in its interior, since any strand crossing it will form an inner monogon
 203 or bigon. Therefore, a minimal monogon can be removed by a single $1 \rightarrow 0$ move.

204 An argument dating back to Steinitz [60, 61] (see Hass and Scott [41, Lemma 1.4]) shows that a
 205 minimal bigon can also be removed using $O(n)$ monotonic moves, where n is the sum of the number of
 206 strands and interior vertices in the bigon.

207 We include the proof to be comprehensive.

208 **Lemma 2.1.** *A non-empty minimal bigon β must have an empty trigon incident to one of the bounding*
 209 *curves. Thus one can first remove all the n vertices inside β using n $3 \rightarrow 3$ moves, followed by removing*
 210 *all s strands of β using s $3 \rightarrow 3$ moves.*

211 **Proof:** Let Θ the tangle formed by γ inside the bigon. Each strand of Θ is simple, otherwise it would
 212 form a monogon, and each pair of strands intersects at most once, otherwise they would form a bigon.
 213 Similarly, each strand intersects two distinct bounding curves. If there are no vertices in this tangle,
 214 there is an empty trigon formed by a vertex and one of the strands.

215 Otherwise, for every vertex x of the tangle obtained by intersecting two strands α and β , the two
 216 strands α and β both intersect one of the bounding curves λ , and thus define a trigon R_x with it. We
 217 denote the other two endpoints by a and b , and look at such a vertex x such that the trigon it defines is
 218 inclusion-wise minimal and one of its three endpoints is on λ . Without loss of generality, a is on λ , and
 219 no strand crosses α between a and x . If a strand crosses β between b and x , denote by y the crossing
 220 point closest to x . This strand does not cross α between a and x , thus R_y is a trigon inside R_x and one
 221 of its endpoints is on λ , which contradicts minimality of R_x . Thus R_x is empty.

222 We can recursively remove the vertices of the tangle Θ using this empty trigon, using n $3 \rightarrow 3$ moves.
 223 Then, using s $3 \rightarrow 3$ moves we can remove all the strands, making the bigon empty. \square

224 This allows us to remove minimal bigons using one last $2 \rightarrow 0$ move. For convenience, we state the
 225 result independently as a lemma, and refer to as the **Steinitz bigon removal algorithm**:

226 **Lemma 2.2.** *Any minimal bigon or monogon with n interior vertices and s strands can be removed*
 227 *using $n + s + 1$ monotonic homotopy moves.*

²In this work, we only care about *embedded* monogons, bigons or trigons and thus only define those. We refer to Hass and Scott [40] for an extensive review of other kinds of monogons and bigons and the corresponding existence results.

2.2 Cut graphs and systems of arcs

A **cellular embedding** of a graph G on a surface Σ is an injective map from G to Σ where all the faces (connected components of complement of the embedding) are homeomorphic to open disks. A **tree-cotree decomposition** of a cellularly embedded graph G is a partition (T, L, C) of the edges of G into three disjoint subsets: a spanning tree T of G , the edges C corresponding to a spanning tree of the dual graph G^* , and exactly $2g$ leftover edges $L := E(G) \setminus (T \cup C)$, where g is the genus of the underlying surface [23]. Let γ be a multicurve on Σ ; we temporarily view γ as a 4-regular graph with some given embedding. However, the embedding of γ is not necessarily cellular; let G be a cellular refinement of γ obtained by triangulating every face. A **dual reduced cut graph** X [24] (hereafter, just **cut graph**) is a cellularly embedded graph obtained from a tree-cotree decomposition (T, L, C) of G as follows: Start with the subgraph of G^* containing the dual spanning tree C^* and the leftover edges L^* , repeatedly delete degree-one vertices, and finally perform series reductions on all vertices with degree two.

The cut graph X inherits a cellular embedding into Σ from the embedding of G^* ; by construction, this embedding has exactly one face. Because every vertex of X has degree 3, Euler's formula implies that X has exactly $4g - 2$ vertices and $6g - 3$ edges. We call the edges of X **arcs**. Cutting the surface Σ along X yields a polygon with $12g - 6$ sides, which we call the **fundamental polygon** of X . The cut graph induces a regular tiling \hat{X} of the universal cover $\hat{\Sigma}$ of Σ ; we refer to each lift of the fundamental polygon of X as a **tile**. By construction, the cut graph X satisfies the following **crossing property**: *Each edge of the curve γ crosses X at most once.*

When Σ is a surface with boundary, it can be cut into a planar piece using exclusively boundary-to-boundary paths: a **system of arcs** Ξ is a collection of simple boundary-to-boundary paths that cuts the surface Σ open into a single polygon. Furthermore, for any closed curve γ on Σ , there exists a system of arcs Ξ satisfying the following **crossing property**: *Each arc in Ξ intersects each edge of γ at most twice, and only transversely.* We summarize this in the following lemma, and refer for example to Colin de Verdière and Erickson [17, Section 6.1] or Erickson and Nayyeri [25, Section 3] for a proof of this, as well as polynomial-time algorithms to compute such Ξ .

Lemma 2.3. *Let Σ be an arbitrary genus- g surface Σ with b boundary components. There is a system of arcs Ξ on Σ of size $O(g + b)$ in general position relative to multicurve γ such that each arc intersects each edge of γ at most twice (and therefore every edge intersects Ξ at most $O(g + b)$ times). Furthermore, Ξ can be computed in $O(n \log n + (g + b)n)$ time, where n is the number of crossings in γ .*

2.3 Hyperbolic trigonometry

We assume the readers have some familiarity with hyperbolic geometry. While we recall most of the properties that we rely on, the hyperbolic intuition is sometimes significantly different from the Euclidean one. We recommend Traver [64] for a nice introduction to hyperbolic trigonometry.

Any surface of negative Euler characteristic can be endowed with a hyperbolic metric. The **area** $A(\Sigma)$ of surface Σ endowed by this metric is constrained related to the Euler characteristic by the Gauss-Bonnet formula: $A(\Sigma) = -2\pi\chi(\Sigma)$. The key hyperbolic property that we will rely on is that any closed curve is homotopic to a unique geodesic under a given hyperbolic metric. When applying this property to a multicurve, we will refer to the collection of geodesics it yields as a **multigeodesic**, or sometimes when there is no ambiguity, simply as a **geodesic**.

The **hyperbolic law of cosines** states that for a geodesic triangle with angles α, β , and γ and side lengths a, b , and c (such that the segment of length a is opposed to the angle α , and similarly for the other ones), we have:

$$\cos \alpha = -\cos \beta \cdot \cos \gamma + \sin \beta \cdot \sin \gamma \cdot \cosh a.$$

A *Saccheri quadrilateral* is a hyperbolic geodesic quadrilateral with two equal sides—called the *legs*—perpendicular to a third side, called the *base*; the fourth side is called the *top*. We denote the lengths of the legs, base, and top as a , b and c , respectively. Any Saccheri quadrilateral satisfies the following property:

$$\sinh \frac{c}{2} = \cosh a \cdot \sinh \frac{b}{2}.$$

A *Lambert quadrilateral* is a hyperbolic geodesic quadrilateral with three right angles. Denoting by α the fourth angle, and by a and b the lengths of the two sides opposite to it, we have the formula

$$\cos \alpha = \sinh a \cdot \sinh b.$$

2.4 Proving the main theorem

We conclude the preliminaries by explaining how to prove Theorem 1.1 assuming Lemmas 1.4 and 1.5:

Proof (of Theorem 1.1): A theorem of Hass and Scott [40, Theorem 2.7] shows that any non-simple *contractible* closed curve on an orientable surface (or more generally, any closed curve homotopic to a simple curve) has an embedded monogon or bigon. Therefore, any multicurve in which a closed curve is contractible and non-simple also contains an embedded bigon or monogon. Note that a simple contractible closed curve crossing other components of the multicurve also forms embedded bigons. Thus after removing all the embedded bigons and monogons using Lemma 2.2—which takes $O(n^2)$ moves for an n -vertex multicurve—we can assume that contractible components, if there are any, have been shrunk to points and removed. Therefore throughout the article, we will assume that there are no contractible components in the multicurves considered. Since any closed curve on a sphere or a disk is contractible, we directly obtain Theorem 1.1 with an $O(n^2)$ bound in such cases.

Lemma 1.4 allows us to reduce the case of boundaryless surfaces (except the torus) to the case of surfaces with boundary. Indeed, once a multicurve has been placed in an ε -neighborhood of its multigeodesic and the neighborhood does not cover the whole surface Σ , one can safely add a puncture (say an arbitrarily small boundary) outside this ε -neighborhood as it has no impact on the tightening of γ . Surfaces with boundary are then dealt with using Lemma 1.5. The case when Σ is a boundaryless torus is not handled by Lemma 1.4 nor by the previous observations, and thus remains untackled in Theorem 1.1. \square

3 Moving Curves Close to Geodesics

In this section we prove Lemma 1.4. Let Θ be a tangle whose disk is endowed with a Riemannian (say hyperbolic or Euclidean) metric so that it is strictly convex. A tangle Θ is *straightened* if all the strands of Θ are shortest paths with respect to the metric. We emphasize the difference between *straightened* and *tightened*: Tightening is a combinatorial condition where all strands are intersecting minimally; straightening is a geometric condition where all strands are shortest paths. A straightened tangle must be tightened. A converse statement is provided by the result of Shepard [58] and Neumann-Coto [50], which says that any multicurve in minimal position on a surface Σ must be shortest paths with respect to some metric on Σ (but not necessarily hyperbolic [42]).

We will make use of the following quantitative version of Ringel’s homotopy theorem [55, 56] (see also [36, 38, 41, 57]). Since none of the earlier results proved the quadratic upper bound, we include a proof below to be comprehensive.

Lemma 3.1 (Hass and Scott [41, Lemma 1.6]). *Any m -vertex tangle Θ can be straightened (with respect to some given metric) monotonically using $O(m^2)$ homotopy moves.*

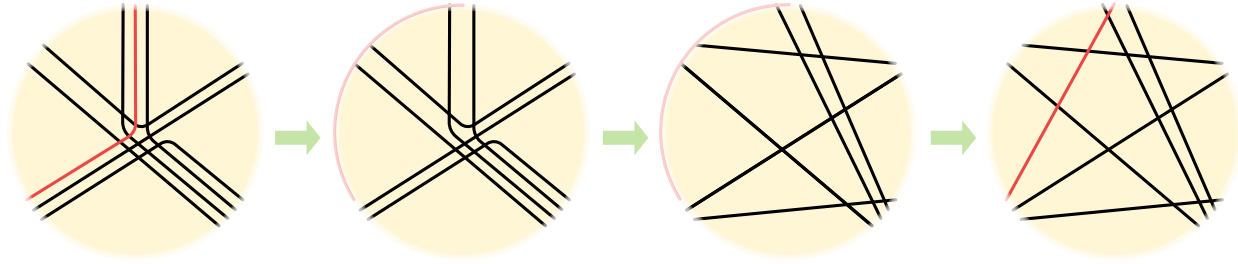


Figure 3.1. The inductive step to straighten a tangle in a Euclidean disk.

313 **Proof:** We denote by $\alpha_1, \dots, \alpha_k$ the strands of a tangle Θ in a disk D , and by $\delta_1, \dots, \delta_k$ the shortest
 314 paths between their endpoints. We will use several times the result of Steinitz's mentioned in Lemma 2.2
 315 in the preliminaries, that any innermost embedded bigon or monogon can be removed using a linear
 316 number of monotonic moves.

317 As a first step, we apply Lemma 2.2 iteratively to any innermost bigon or monogon in the tangle Θ .
 318 Since removing a bigon or monogon reduces the number of vertices by at least one, this can be done in
 319 $O(m^2)$ moves, after which there are no embedded bigons nor monogons in Θ anymore. In particular,
 320 every strand α_i is simple and any pair of strands α_i and α_j crosses at most once (at this point, the tangle
 321 Θ is tightened but not *straightened*).

322 The remainder of the proof uses induction on the number of strands in the tangle. The base case is
 323 trivial: a tangle made of a single strand can be straightened without using any move. Inductive step is
 324 pictured in Figure 3.1.

325 For an s -strand tangle Θ , we consider the bigons formed by one subpath of a strand and a subpath
 326 of the disk boundary ∂D . Since all strands are simple and all bigons between any two strands of Θ
 327 were removed, we can find a bigon between some α_i and ∂D that is innermost. Such a bigon is only
 328 crossed transversely by other strands of the tangles and its vertices can be removed using $O(m)$ $3 \rightarrow 3$
 329 moves by applying the first step of Lemma 2.1. Once the bigon contains no vertices, we can move α_i
 330 towards ∂D until α_i is arbitrarily close to ∂D . One can then consider a slightly smaller disk than D that
 331 contains all the strands of the tangle Θ except α_i . The new tangle defined by the smaller disk is then
 332 straightened recursively. Then, what remains is to move α_i to the shortest path δ_i . Since shortest paths
 333 cross minimally, they do not form bigons. And because α_i was chosen so that the bigon formed with
 334 a subpath of ∂D was innermost, as all the other strands have been straightened inductively, the bigon
 335 between α_i and δ_i must be innermost, and can be swept using $O(m)$ moves again by Lemma 2.2. Note
 336 that if α_i does not cross any other strand of Θ , this inductive step costs zero moves. The total number of
 337 moves used throughout the recursion is therefore $O(s' \cdot m)$, where s' is the number of strands crossing
 338 at least some other strand. By charging each of these strands to one of their crossing points, we have
 339 $s' = O(m)$, and therefore the total bound on number of moves is $O(m^2)$. \square

340 We will use the following corollary of Lemma 3.1 in subsequent sections.

341 **Corollary 3.2.** *Let δ be a trigon with m vertices. Trigon δ can be made empty using $O(m^2)$ monotonic
 342 homotopy moves in a small neighborhood of δ .*

343 **Proof:** Consider the tangle Θ formed by taking a small neighborhood of the trigon δ . We endow Θ with
 344 a metric in such a way that the trigon, formed by replacing the three strands that are the bounding
 345 curves of δ with shortest paths with respect to the metric, has its orientation opposite to that of δ . To
 346 see the existence of such metric, first we endow Θ with a metric of constant curvature (say a hyperbolic
 347 metric). Notice that by deforming the distances within a small neighborhood of the disk boundary we

348 can realize arbitrary spacings between endpoints of the strands. Now by placing the endpoints of the
 349 three bounding curves of δ carefully and connecting each pair of them using shortest paths (with respect
 350 to the endowed metric of constant curvature), one can realize either orientation of the trigon. Applying
 351 Lemma 3.1 to Θ with respect to the constructed metric empties and flips the trigon δ in $O(m^2)$ moves;
 352 we terminate the algorithm just before δ is flipped. \square

353 3.1 Constructing the hyperbolic metric

354 In this subsection, we explain how to endow Σ with a hyperbolic metric that is well-tailored to the
 355 purpose of tightening γ .

356 **Lemma 3.3.** *Let Σ be a boundaryless surface of genus $g \geq 2$ and γ be an n -vertex non-contractible
 357 multicurve on Σ . There is a **hyperbolic metric** d_H on Σ such that*

- 358 (1) *multicurve γ can be turned into another multicurve γ' of length $O(n \log g)$ using $O(n^2)$ monotonic
 359 homotopy moves, and*
 360 (2) *the length of the shortest non-contractible cycle on Σ (known as the systole) is at least 1.*

361 **Proof:** The construction is similar to the argument in Dehn's seminal result [20] that the graph distance
 362 on a regular tiling of the universal cover $\hat{\Sigma}$ approximates the hyperbolic metric on $\hat{\Sigma}$. Construct a
 363 cut graph X from the curve γ such that every edge of γ crosses X at most $O(1)$ times, as described in
 364 Section 2.2. Lift the cut graph X to the universal cover endowed with the unique hyperbolic metric, such
 365 that the edges of X are geodesic segments of equal length and each corner has angle $1/3$ circles; this
 366 implies, using the hyperbolic law of cosines, that each side of the fundamental polygon has length at
 367 least 1.³ Note that the diameter of the fundamental polygon is $O(\log g)$, which also follows from the
 368 hyperbolic law of cosines. One can project the metric back to the original surface; denote the hyperbolic
 369 metric constructed as d_H .

370 To prove that the hyperbolic metric d_H defined on surface Σ satisfies item (1), consider the modified
 371 curve γ' where all strands within the open disk $\Sigma \setminus X$ are straightened using Lemma 3.1. As per lemma,
 372 γ' can be obtained from γ using $O(n^2)$ moves. Note that any geodesic path not intersecting X has length
 373 at most the diameter of the fundamental polygon with respect to d_H , which is $O(\log g)$. This directly
 374 implies that the length of γ' is at most $O(n \log g)$, thus the hyperbolic metric d_H satisfies item (1).

375 As for item (2), consider any non-contractible cycle σ on surface Σ ; without loss of generality assume
 376 σ to be a geodesic. If we lift σ to the universal cover $\hat{\Sigma}$ such that the lift $\hat{\sigma}$ starts and ends on the lift \hat{X}
 377 of the cut graph X , because σ is non-contractible, the two arcs of \hat{X} where $\hat{\sigma}$ starts and ends respectively
 378 are two different translates of the same arc in X . Consider the sequence of arcs a_0, \dots, a_k in \hat{X} intersected
 379 by $\hat{\sigma}$. Because σ is a geodesic and every vertex in \hat{X} has degree 3, one has $a_i \neq a_{i+1}$ and no a_i is incident
 380 to a_{i+2} for all i . If for some i the two arcs a_i and a_{i+1} are not incident to each other (that is, a_i and a_{i+1}
 381 do not share a vertex in \hat{X}), then by hyperbolic trigonometry the length of the subpath of $\hat{\sigma}$ connecting
 382 a_i to a_{i+1} is at least the length of the side of the polygon, which is at least 1. Otherwise, if a_i is incident
 383 to a_{i+1} and a_{i+1} is incident to a_{i+2} , as a_i is not incident to a_{i+2} , by reflecting the subpath of $\hat{\sigma}$ from a_{i+1}
 384 to a_{i+2} to the tile that contains a_i and a_{i+1} we again have the length of the subpath from a_i to a_{i+1} of $\hat{\sigma}$
 385 lower-bounded by the length of a_{i+1} . This proves that d_H satisfies item (2). \square

386 3.2 Straightening multicurve using disks

387 **Tortuosity.** Let γ be a multicurve on Σ . Denote $D(x, r)$ the disk centered at point x with radius r
 388 (with respect to the constructed metric d_H in Lemma 3.3). Denote the two endpoints of the maximal

³To be accurate, the side length is equal to $2 \cosh^{-1}(\sin(2\pi/6) \cdot \cos(2\pi/(24g - 12)))$ which is bigger than 1 for all $g \geq 2$.

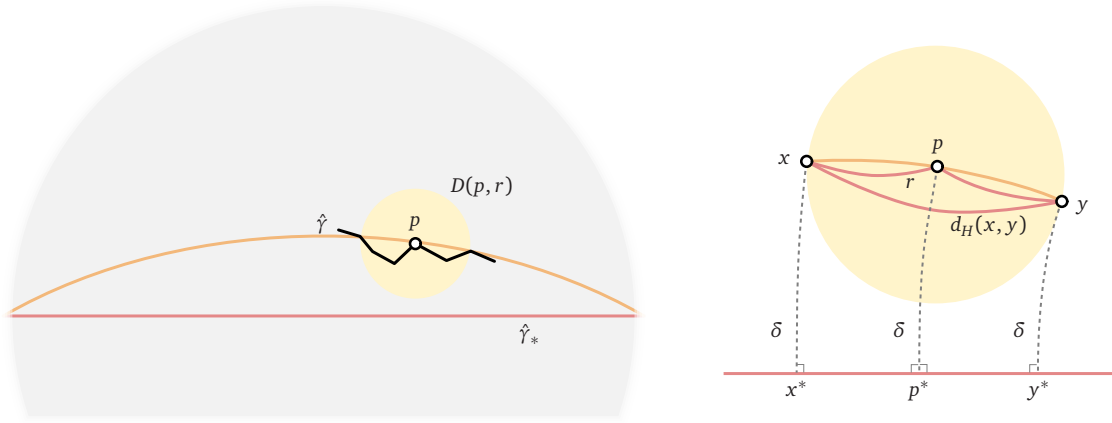


Figure 3.2. Left: The setup for proof of Lemma 3.4, represented in the Poincaré disk model. The orange curve is the set of points at distance exactly δ from $\hat{\gamma}_*$. This *hypercircle* is not a geodesic, but is always a circular arc in the Poincaré disk. Right: Zooming around the disk $D(p, r)$. The tortuosity is minimized when x and y lie on the orange hypercircle. The geodesics between x , p , and y are in red, and three Saccheri quadrilaterals are formed by red and dotted geodesic arcs.

389 subpath of γ in $D(\gamma(t), 1/2)$ containing $\gamma(t)$ as x and y , and the maximal subpath itself as $\gamma[x, y]$. The
 390 **tortuosity** [38] of the multicurve γ at point t , denoted as $\mathbf{tort}(\gamma, t)$, is the difference between the length
 391 of the subpath of γ lying in $D(\gamma(t), 1/2)$ and the geodesic distance between the two endpoints of the
 392 subpath:

$$393 \quad \mathbf{tort}(\gamma, t) := \text{len}(\gamma[x, y]) - d_H(x, y).$$

394 In practice, the tortuosity of γ at point t lower bounds the improvement one will make after straightening
 395 the disk $D(\gamma(t), 1/2)$. The tortuosity of a multicurve γ is the supremum of $\mathbf{tort}(\gamma, t)$ where t ranges over
 396 $[0, 1]$. The goal of the following lemma is to prove that when the tortuosity of a multicurve is small,
 397 then the whole multicurve is ε -close to its multigeodesic. In other words, as long as the multicurve γ has
 398 points that are at least ε away from the geodesic, we can always find a disk centered at some point of γ
 399 whose straightening will decrease the length of γ by at least fixed amount, depending only on ε .

400 **Lemma 3.4.** *For any $\varepsilon > 0$ smaller than the systole of Σ , if the tortuosity of γ is at most $O(\varepsilon^2)$, then γ is*
 401 *ε -close to the multigeodesic γ_* .*

402 **Proof:** We will prove the contrapositive statement using hyperbolic trigonometry. For the sake of
 403 generality we temporarily treat r as a variable; at the end of the calculation one just plugs in $r := 1/2$.
 404 Here we list two identities that will be used in our proof.

405 (1) For any real number x , $\sinh(2x) = 2 \sinh x \cosh x$ and $(\cosh(x))^2 - (\sinh(x))^2 = 1$.

406 (2) Given an arbitrary *Saccheri quadrilateral* with the lengths of the legs, base, and top as a , b , and c
 407 respectively, then

$$408 \quad \sinh \frac{c}{2} = \cosh a \cdot \sinh \frac{b}{2}.$$

409 Lift both γ and γ_* to the universal cover $\hat{\Sigma}$; denote the resulting families of paths as $\hat{\gamma}$ and $\hat{\gamma}_*$
 410 accordingly. Let t be a point in $[0, 1]$ such that $\hat{\gamma}(t)$ has maximum distance to $\hat{\gamma}_*$. Refer to point $\hat{\gamma}(t)$ as
 411 p and the maximum distance as δ ; by assumption δ is at least ε . Our goal is to prove that the tortuosity
 412 of γ at t is at least $\Omega(\varepsilon^2)$. One has

$$413 \quad \mathbf{tort}(\gamma, t) = \text{len}(\hat{\gamma}[x, y]) - d_H(x, y) \geq 2r - d_H(x, y).$$

414 Here without loss of generality we will assume that x and y are both at distance exactly δ to $\hat{\gamma}_*$. The
 415 reason one can make such an assumption is that, as one moves x and y perpendicularly along the
 416 geodesics away from $\hat{\gamma}_*$, $d_H(x, y)$ increases and therefore the tortuosity when both x and y are at
 417 distance δ is a lower bound to the original tortuosity. See Figure 3.2.

418 What is left is to upper bound $d_H(x, y)$. Let x^* , p^* , and y^* be the points on $\hat{\gamma}_*$ that have minimum
 419 distance to x , p , and y respectively. By identity (2) one has

$$420 \quad \sinh(d_H(x, y)/2) = \cosh \delta \cdot \sinh(d_H(x^*, y^*)/2)$$

421 and

$$422 \quad \sinh(r/2) = \cosh \delta \cdot \sinh(d_H(x^*, y^*)/4).$$

423 The second equality gives us

$$424 \quad d_H(x^*, y^*)/2 = 2 \sinh^{-1} \left(\frac{\sinh(r/2)}{\cosh \delta} \right),$$

425 which we plug back in the first equation to get

$$426 \quad \sinh(d_H(x, y)/2) = \cosh \delta \cdot \sinh \left(2 \sinh^{-1} \left(\frac{\sinh(r/2)}{\cosh \delta} \right) \right).$$

427 Apply identity (1) on the first hyperbolic sine, one has

$$\begin{aligned} 428 \quad \sinh(d_H(x, y)/2) &= \cosh \delta \cdot 2 \cdot \sinh \left(\sinh^{-1} \left(\frac{\sinh(r/2)}{\cosh \delta} \right) \right) \cdot \cosh \left(\sinh^{-1} \left(\frac{\sinh(r/2)}{\cosh \delta} \right) \right) \\ 429 \quad &= \cosh \delta \cdot 2 \cdot \left(\frac{\sinh(r/2)}{\cosh \delta} \right) \cdot \cosh \left(\sinh^{-1} \left(\frac{\sinh(r/2)}{\cosh \delta} \right) \right) \\ 430 \quad &= 2 \cdot \sinh(r/2) \cdot \left(1 + \left(\sinh \left(\sinh^{-1} \left(\frac{\sinh(r/2)}{\cosh \delta} \right) \right) \right)^2 \right)^{1/2} \\ 431 \quad &= 2 \cdot \sinh(r/2) \cdot \left(1 + \left(\frac{\sinh(r/2)}{\cosh \delta} \right)^2 \right)^{1/2}. \end{aligned}$$

433 This shows that

$$434 \quad d_H(x, y) = 2 \cdot \sinh^{-1} \left(2 \cdot \sinh(r/2) \cdot \left(1 + \left(\frac{\sinh(r/2)}{\cosh \delta} \right)^2 \right)^{1/2} \right).$$

436 Taylor expand $d_H(x, y)$ around $\delta = 0$ gives us

$$437 \quad d_H(x, y) = 2r - \frac{(\sinh(r/2))^3}{\cosh(r/2) \cdot \cosh(r)} \delta^2 + O(\delta^4),$$

438 and therefore $\text{tort}(\gamma, t) \geq \Omega(\delta^2) \geq \Omega(\varepsilon^2)$. □

439 Let us emphasize here how resolutely hyperbolic this lemma is. It works because a line equidistant
 440 to a geodesic (here $\hat{\gamma}_*$) is *not* a geodesic in hyperbolic geometry, and it is this defect of geodesicity that
 441 we exploit to lower bound the tortuosity. Comparatively, in Euclidean geometry, a line equidistant to
 442 a straight line is again a straight line, and thus there is no analogue lemma. This is why our proof
 443 techniques do not apply to the boundaryless torus.

444 **Exposing points outside the neighborhood.** Now we proceed to upper bound ε so that the ε -
445 neighborhood of the multigeodesic γ_* does not cover the whole surface Σ .

446 **Lemma 3.5.** *Let γ be an n -vertex multicurve on Σ . Then the ε -neighborhood of γ_* does not cover the
447 whole surface Σ if ε is at most $O(g/(n \log g))$.*

448 **Proof:** Given any multicurve γ with the corresponding multigeodesic γ_* on the surface Σ with the
449 constructed hyperbolic metric d_H , the length of γ_* is at most $O(n \log g)$ by Lemma 3.3(1). For small
450 enough ε , the area of the ε -neighborhood of a multicurve with length ℓ is at most $O(\varepsilon \ell)$. To see this,
451 cover the neighborhood with kite-like *Lambert quadrilaterals* with length of the short sides as ε . The only
452 acute angle α of the quadrilateral is equal to $\arccos((\sinh \varepsilon)^2)$. The area of the quadrilateral is equal to
453 the angle deficit, which is $\pi/2 - \alpha$. Therefore the area of the quadrilateral is at most $O(\varepsilon^2)$, and thus the
454 total area of the ε -neighborhood on Σ is at most $O(\varepsilon^2 \cdot \ell / \varepsilon) = O(\varepsilon \ell)$.

455 The area of the surface is precisely $(4g - 4)\pi$. (This follows directly from the Gauss-Bonnet theorem
456 which is independent of the hyperbolic metric up to scaling.⁴) This implies that for the ε -neighborhood
457 of γ_* to cover the whole surface Σ , the following holds:

$$458 \quad \varepsilon \geq \frac{(4g - 4)\pi}{O(n \log g)} \geq \Omega\left(\frac{g}{n \log g}\right).$$

459 In other words, if we set $\varepsilon \leq O(g/(n \log g))$, then the ε -neighborhood of γ_* cannot cover the whole
460 surface Σ , thus proving the lemma. \square

461 Basmajian, Parlier, and Souto [8] showed that for any fixed genus g , the $O(1/n)$ bound in Lemma 3.5
462 is tight up to logarithmic factors.

463 3.3 Putting it together

464 Now we are ready to prove Lemma 1.4.

465 **Proof (of Lemma 1.4):** We use Lemma 3.3 to endow Σ with a hyperbolic metric. By Lemma 3.3(1),
466 after applying $O(n^2)$ monotonic homotopy moves the resulting multicurve γ' has length $O(n \log g)$.
467 Consider the set of disks centered at each point on the multicurve with radius $1/2$, which is smaller than
468 half the systole by Lemma 3.3(2); therefore all such disks are embedded in Σ . Straighten any disk using
469 Lemma 3.1 if the tortuosity of the center point is at least ε^2 . Once every point on γ' has tortuosity less
470 than ε^2 , by Lemma 3.4 the multicurve γ' now lies in the ε -neighborhood of γ_* .

471 Straightening a disk takes $O(n^2)$ moves using Lemma 3.1. The tortuosity at a center of each disk is a
472 lower bound on the difference between the lengths of the multicurve γ' before and after straightening.
473 From Lemma 3.3(1) the length of γ' is at most $O(n \log g)$. Every time a disk is straightened the length of
474 γ' will drop by at least ε^2 . Since γ' is non-contractible, the length of any curve homotopic to γ' is at least
475 the systole, which is $\Omega(1)$ by Lemma 3.3(2). Therefore at most $O(n \log g / \varepsilon^2)$ disks will be straightened
476 before every point has tortuosity less than ε^2 . In total at most $O(n^3 \log g / \varepsilon^2)$ homotopy moves are
477 performed. From Lemma 3.5, setting $\varepsilon := \Theta(g/(n \log g))$ concludes the proof of Lemma 1.4. \square

⁴Alternatively, one can derive the area directly: divide the fundamental polygon into $12g - 6$ triangles by drawing straight-lines from the center of the polygon to all vertices, and use the area formula for triangles.

4 Tightening Curves on Surface with Boundary

In this section we prove Lemma 1.5. Throughout the rest of the section, let Σ be an orientable surface with boundary and let γ be a multicurve on Σ .

The second phase of the curve shortening algorithm by de Graaf and Schrijver [38] starts with a multicurve γ lying within an ε -neighborhood of its multigeodesic on Σ , where in some cases ε is required to be exponentially small. Unfortunately we cannot afford to drag γ exponentially close to its geodesic which requires more than polynomially many moves (Section 3). Instead, we make the observation that one can mimic this part of the algorithm in a combinatorial way, which, in particular, does not require the multicurve γ to be close to its own geodesic. We pick an open neighborhood—called a *pipe system*—of some underlying skeleton graph, such that γ can be drawn in proper ways respecting the pipe system. We then describe a way to morph the pipe systems using *cluster* and *pipe expansions*, a technique introduced by Cortese *et al.* [19] in graph drawings (and later on applied to weak embeddings [2, 3, 15] and crossing numbers [30]), so that the multicurve inside the pipe system can be canonicalized using polynomially many monotonic homotopy moves. Conceptually the expansion operations can be viewed as ways to morph the metric on surface Σ , so that curves on Σ get transformed closer and closer to the geodesic with respect to the morphing metric. After γ is canonical we use the crossing minimization algorithm for flat braids to tighten γ [32, 38].

We first define an initial pipe system using system of arcs, and the multicurve is then made to respect the pipe system in Section 4.1. In Section 4.2 we introduce the expansion operations formally, followed by a description of the main algorithm and its analysis in Section 4.3.

4.1 Putting Curves into a Pipe System

Let G be a (multi-)graph drawn on a surface Σ with boundary; we refer to the vertices and edges of G as *clusters* and *pipes*. The drawing of G is not necessarily an embedding; assume without loss of generality that all self-intersections of G are between its edges, are transverse and involve at most two edges. A *pipe system* Π^5 of G is a topological neighborhood of the drawing of G on surface Σ with a decomposition into regions corresponding to clusters and pipes.

- For each cluster u in G , a *cluster region* D_u is a topological disk containing u .
- For each pipe uv in G , a *pipe region* R_{uv} is a topological disk containing uv that is disjoint from the interior of the cluster regions D_u and D_v . Notice that if two pipes intersect in the drawing of G , then the two corresponding pipe regions cross on the surface Σ . However, three pipe regions are never allowed to overlap at any common point.
- For each cluster u , there are disjoint connected subsets of the boundary of D_u forming *ends* $A_{u,v}$, one for each incident edge uv , in the order of the rotation system defined by the drawing of G ; identify the intersection between D_u and R_{uv} with $A_{u,v}$.

When there is no risk of confusion, we sometimes refer to cluster and pipe regions as clusters and pipes as well. Let Π be the collection of all the cluster and pipe regions; from time to time we also abuse the notation and refer to the *union* of all cluster and pipe regions as Π , so that one can safely use sentences like “(part of) γ lies in the pipe system Π ”. If pipe system Π is constructed from graph G , we refer to G along with its drawing as the *skeleton* of Π . Each region can be viewed as a tangle; a *strand* of a cluster or pipe is a maximal subpath of γ inside the corresponding region.

It is easier to talk about the pipe system by imposing geometry to the topological disks: throughout this section, we will generally endow the cluster regions D_u with the metric of a Euclidean disk, and the

⁵also known as strip system [3, 15] or thickening [30]

520 pipe regions R_{uv} with the metric of a thin Euclidean rectangle. However we emphasize that while some
 521 constructions and proofs in the following sections are described using geometry, they can be rephrased
 522 using purely combinatorial languages.

523 Now the plan is to construct an initial pipe system Π_0 using the system of arcs from Lemma 2.3. Let
 524 Ξ denote the system of arcs given by Lemma 2.3. The **pipe system** Π_0 is obtained by taking the dual
 525 graph of Ξ as a skeleton graph G , which consists of one unique cluster and $O(g + b)$ (self-loop) pipes.
 526 But since we care about its precise position with respect to γ , we need to describe the construction of
 527 Π_0 more carefully. We replace each arc of Ξ by two identical copies infinitesimally close to each other,
 528 co-bounding a 4-gon with two infinitesimal subpaths of the boundary. Each of these 4-gons is a pipe of
 529 the pipe system Π_0 while the “big” component corresponding to the unique polygon obtained by cutting
 530 Σ along Ξ is the single cluster of Π_0 . Note that γ is trivially contained in the union of the regions of this
 531 pipe system, since this union is the whole surface Σ .

532 We will prove in Lemma 4.2 that the multicurve γ can be made to *respect* Π_0 by satisfying some good
 533 properties. Such modified γ along with the pipe system Π_0 will be the starting point of the algorithm.

534 **Respecting pipe system.** We say that a multicurve γ *respects* a given pipe system Π if

- 535 (1) γ lies completely in Π ;
- 536 (2) all strands in any cluster or pipe region are simple and no two strands intersects more than once;
- 537 (3) each component of the intersection between γ and any end of Π is a single transverse crossing;
- 538 (4) γ never intersects the same end consecutively more than once; in other words, whenever a curve
 539 enters a topological disk (whether it's a cluster or pipe region) from one end, the curve must leave
 540 from another end of the disk; and
- 541 (5) within the intersection of a pair of pipe regions, pairs of strands from the same pipe region are not
 542 allowed to cross.

543 Before we continue, we quickly comment that given any multicurve γ respecting a pipe system, one
 544 can safely assume the following additional property as part of the definition.

- 545 (6) No intersections of γ are between strands of the same pipe.

546 **Lemma 4.1.** *Let Π be a pipe system. Let R be a pipe region of Π , which is crossed transversely by other
 547 pipe regions R_1, \dots, R_k . Let γ be a multicurve with n crossings respecting Π , but the strands of γ may
 548 cross in the pipes. Then one can find a sequence of $O(|R|^2)$ monotonic homotopy moves to push all the
 549 crossings between strands of R to an incident cluster region, where $|R|$ denotes the number of crossings
 550 between strands of R .*

551 **Proof:** We will push the crossings between strands of R into an incident cluster region using a controlled
 552 number of $3 \rightarrow 3$ moves. A crossing between two strands of R is called *extremal* if, out of the four substrands
 553 that it defines, two of those do not cross any other strand of R and end at the same end of R . Pick such
 554 an extremal crossing z between two strands inside R : by orienting R and its strands from one end to
 555 the other, leftmost and rightmost crossings will be extremal because of Properties (2) and (4). Now,
 556 the obstruction to simply moving z to an incident cluster comes from the other pipe regions crossing R
 557 transversely, as their strands stand in the way. As part of the definition of a pipe system, no two pipe
 558 regions R_i and R_j intersects R at a common point.

559 By Property (5), the strands of these transverse pipe regions do not cross within the intersection.
 560 Thus, the crossing z can be pushed past strands of transverse pipes using only $3 \rightarrow 3$ moves. See Figure 4.1.
 561 Since there are $O(|R|)$ crossings to push and each is pushed past $O(n)$ strands from transverse pipes (since
 562 each transverse strand induces at least once crossing), this can be done using $O(n^2)$ $3 \rightarrow 3$ moves. \square

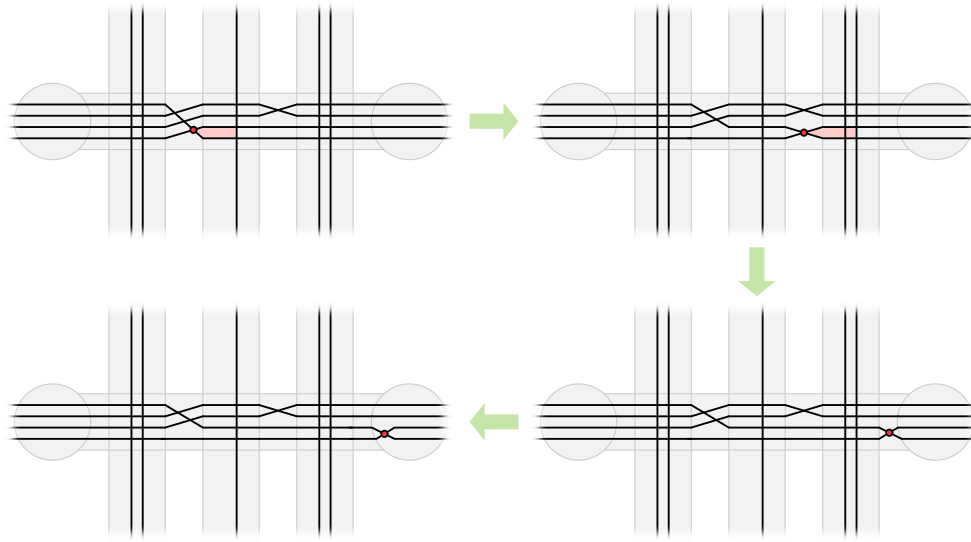


Figure 4.1. The red crossing within a pipe is pushed towards an incident cluster by doing 3→3 moves on the triangles marked in pink.

563 Using this lemma on all the pipe regions costs $O(n^2)$ moves. Observe that all crossings of a multicurve
 564 γ respecting a pipe system must either be inside the clusters, or between two intersecting pipes where
 565 the strands of the two pipes intersect in a grid-like pattern. The strands inside a pipe can be drawn in
 566 parallel connecting from one end to the other, preserving their order on each end.

567 **Closed walks on skeleton graph.** If a multicurve γ respects a pipe system Π whose skeleton graph is
 568 G , one can define **closed walks** C associated with γ on G as follows. Let γ_i be one of the constituent
 569 curve of γ . Let

$$570 A_{u_0, u_1}, A_{u_1, u_0}, A_{u_1, u_2}, A_{u_2, u_1}, \dots, A_{u_{w-1}, u_0}, A_{u_0, u_{w-1}}$$

571 be the sequence of ends of Π that γ_i intersects. Then closed walk $C_{\Pi}(\gamma_i)$ in G is defined to be

$$572 [u_0, u_1, \dots, u_{w-1}, u_0].$$

573 Closed walks are considered without basepoint, that is, up to cyclic permutations. Closed walks $C_{\Pi}(\gamma)$
 574 are defined to be the collection of all closed walks $C_{\Pi}(\gamma_i)$, each corresponding to a constituent curve
 575 γ_i of γ . Let $C(u)$ and $C(uv)$ denote the vertices and edges of closed walks C that correspond to the
 576 cluster u and pipe uv , respectively. Let the **weight** $n(uv)$ be the number of times C uses pipe uv in
 577 G (in either direction); one has $n(uv) = |C(uv)|$. Observe that the closed walks C do not contain any
 578 *spurs*—subwalks of the form $[u, v, u]$ —by Property (4) in the definition of respecting a pipe system.

579 Now we show that any multicurve γ lying in the initial pipe system Π_0 can be made to respect it
 580 using a polynomial number of monotonic homotopy moves.

581 **Lemma 4.2.** *Let Σ be a genus- g orientable surface with b boundary components. Any multicurve γ on*
 582 *Σ with n crossings can be made to respect the pipe system Π_0 using $O((g + b)n^2)$ monotonic homotopy*
 583 *moves. Furthermore, the tightening problem remains unchanged: any tightening of γ' within the pipe*
 584 *system is also a tightening of γ . The length of the closed walk C corresponding to γ on G is at most*
 585 *$O((g + b)n)$.*

Proof: The very first step is to modify γ so that it contains no embedded monogons or embedded bigons within Π_0 . This step follows from Steinitz algorithm (Lemma 2.2) and takes $O(n^2)$ moves, since removing each bigon or monogon takes $O(n)$ moves and this may need to be done $O(n)$ times.

We then use $O(|\gamma \cap \Pi_0| \cdot n)$ monotonic homotopy moves to ensure that γ does not form any bigon with any end of Π_0 . This is identical to the first step in Chang *et al.* [13, Lemma 4.4]; we repeat the main idea for clarity. Assuming that there exists such a bigon, let B denote a minimal embedded bigon (under containment) between γ and an end of Π_0 . By minimality, the only subpaths of γ occurring inside B have to be simple and crosses B transversely, from one side to the other. Thus, we can remove B by moving the subpath of γ bounding B across, going over each vertex one by one with a $3 \rightarrow 3$ move. We refer to Lemma 4.4 of Chang *et al.* [13] for more details and an illustration of this process. Removing all the bigons between γ and the ends of Π_0 using this technique costs $O(|\gamma \cap \Pi_0| \cdot n)$ monotonic homotopy moves.

We immediately have Property (1) because γ is contained in the union of the regions of Π_0 . Property (2) follows from the fact that we first tightened γ to remove embedded monogons and bigons: if any strand of α was non-simple in a cluster or a pipe, it would form such a monogon or bigon. Since γ crosses the ends of Π_0 transversely, the crossings between γ and any end of Π_0 is a point, yielding Property (3). We removed bigons between the ends Π_0 and γ , and thus γ cannot intersect the same end of Π_0 consecutively more than once as it would yield a bigon. This gives Property (4). Property (5) is true as the interiors of different pipe regions of Π_0 do not intersect.

As all the homotopy moves are performed within the pipe system Π_0 , any tightening that can be obtained from the original γ on the surface Σ can also be realized by a tightening of the new γ within Π_0 that covers the whole Σ . Furthermore, based on the fact that each edge of γ intersects Ξ only $O(g + b)$ times, the length of the closed walks C constructed from γ will be at most $O((g + b)n)$. Thus γ can be made to respect Π_0 using $O(|\gamma \cap \Pi_0| \cdot n + n^2) = O((g + b)n^2)$ monotonic homotopy moves. \square

4.2 Tightening curves using local operations

We define two operations called the *cluster expansion* and *pipe expansion* performed on a multicurve γ lying in a pipe system Π in this subsection. Such operations have been used to study clustered planarity in graph drawings [19, 31], weakly simple polygons [2, 15], weak embeddings of graphs [3], and crossing numbers [30]. Our definition most closely resembles the one in Fulek and Tóth [30]; both allow the edges of skeleton graph G to cross in the drawing. The main differences are, instead of preserving crossing numbers, we need to argue that the tightening problem remains the same before and after the expansion; and unlike the previous papers where expansions can be done instantly, we have to implement each expansion operation using monotonic homotopy moves. While the constructions are described geometrically, the exact shape and position of the regions are mostly artificial and irrelevant; the only important thing is the change to the combinatorial structure.

Cluster expansion. We perform the following *cluster expansion* on cluster u and its region D_u in a pipe system Π with skeleton graph G . To describe the construction, we endow D_u with Euclidean metric such that all the ends are infinitesimally small, and position these ends so that there are no triple intersecting strands of D_u .

We modify γ by replacing every strand of D_u with a straight line, and modify G and Π accordingly (see Figure 4.2): For each pipe uv incident to u , create a new cluster $[uv]$, whose corresponding cluster region in Π is an elliptical neighborhood of the end $A_{u,v}$, and rename the pipe uv to $[uv]v$. For every pair of pipes uv and uw in G insert a pipe $[uv][uw]$ if there was a strand of γ that connects the end $A_{u,v}$ with the end $A_{u,w}$; insert the corresponding rectangular pipe regions in Π accordingly, so that in the drawing of G and Π the pipes intersect transversely. By the choice of Euclidean metric on D_u , these pipe regions

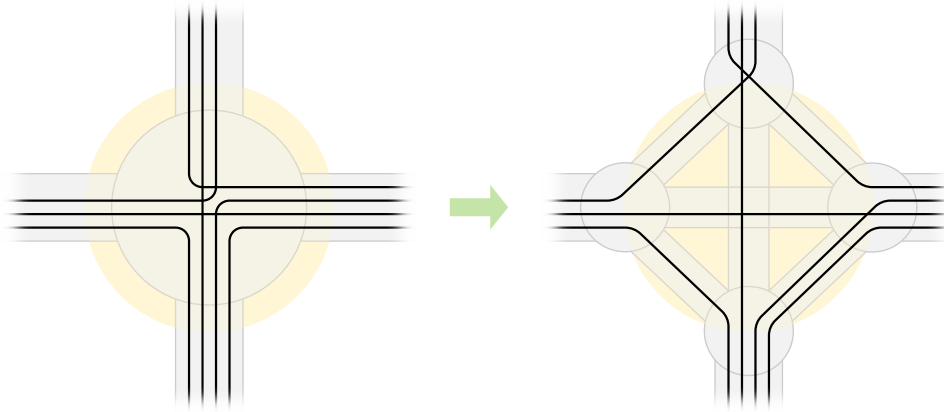


Figure 4.2. Expanding a cluster D_u . The infinitesimal ends have been widened for visibility.

631 can be taken to be arbitrarily thin and so that no three of them overlap at a point. Finally, remove cluster
 632 u from G and region D_u from Π . Denote the multicurve and pipe system after cluster expansion as $\tilde{\gamma}$ and
 633 $\tilde{\Pi}$, respectively.

634 **Lemma 4.3.** *First, the cluster expansion can be implemented using $O(n^2)$ monotonic homotopy moves,*
 635 *such that after cluster expansion the new multicurve $\tilde{\gamma}$ still respects the modified pipe system $\tilde{\Pi}$. Second,*
 636 *if we denote by $\tilde{\gamma}_*$ any tightening of $\tilde{\gamma}$ within the modified pipe system $\tilde{\Pi}$ (viewed as a topological space),*
 637 *then $\tilde{\gamma}_*$ is also a tightening of γ within Π .*

638 **Proof:** Conceptually, this can be implemented by straightening the tangle defined by the cluster region
 639 using Lemma 3.1 in $O(n^2)$ moves, as the number of crossings in γ is upper bounded by n at any point of
 640 the algorithm because the homotopy process is monotone.

641 Next we prove that the modified multicurve $\tilde{\gamma}$ respects the modified pipe system $\tilde{\Pi}$, by showing
 642 Properties (1)–(5) (and thus also (6)). Let the cluster expansion be performed on cluster u . Properties (1)–
 643 (3) immediately follow from the new strands being straight lines and the disk being convex. For
 644 Property (4), consider ends of two different types: ends of the form $A_{[uv],v}$ and ends of the form $A_{[uv],[uw]}$,
 645 where v and w are clusters adjacent to u in G . For ends of the first type, if γ intersects $A_{[uv],v}$ consecutively
 646 twice, the subpath of γ between the two intersections must lie inside D_u , and therefore must be a strand
 647 in D_u . This implies that γ did not respect Π as Property (4) was already violated, a contradiction. For
 648 ends of the second type, as we took the new clusters to be elliptical neighborhoods of the ends, and
 649 the new strands are all straight lines between the ends, each such strand can cross the boundary of
 650 each cluster of $\tilde{\Pi}$ at most once. Property (5) follows from the fact that the pipe regions can be made
 651 infinitesimally thin, and thus generically there are no crossings within the intersection of two of those.

652 The second item of the lemma is a consequence of the facts that the cluster expansion performed on
 653 two multicurves with identical closed walks in the skeleton graph before expansion creates two new
 654 multicurves with identical closed walks in the new skeleton graph after expansion, and that homotopy
 655 between two multicurves within the pipe system is equivalent to the *equality* between two corresponding
 656 closed walks in the skeleton graph.

657 More in details. Since, as a topological space, $\tilde{\Pi}$ is obtained from Π by adding punctures, any
 658 tightening $\tilde{\gamma}_*$ of $\tilde{\gamma}$ within $\tilde{\Pi}$ is also homotopic to $\tilde{\gamma}$ (and thus to γ) within Π . So it suffices to prove that
 659 such a $\tilde{\gamma}_*$ is tight within Π . In order to do so, let γ_* denote a tightening of γ within Π ; we prove that γ_*
 660 and $\tilde{\gamma}_*$ have equally many self-crossings.

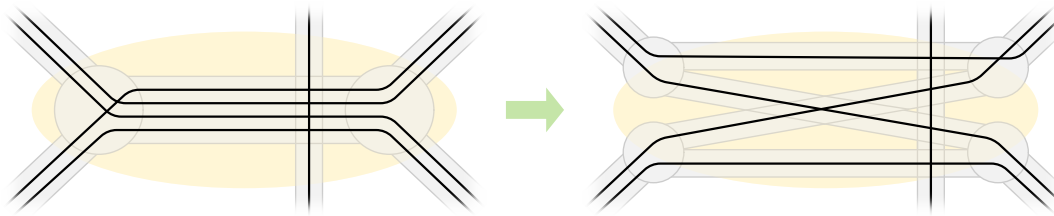


Figure 4.3. Expanding a pipe R_{uv} . The infinitesimal ends have been widened for visibility.

661 First we claim that γ_* can be made to respect the pipe system Π using monotonic homotopy moves
 662 (no matter how many). The proof follows closely the one of Lemma 4.2. As γ_* is tight, it contains no
 663 embedded monogons or bigons. We ensure that it does not form any bigon with any end of Π by undoing
 664 such bigons, starting from the innermost ones. As in that proof, γ_* now satisfies Properties (1)–(4), but
 665 it may fail to satisfy Property (5). Within the intersection of two pipe regions, if two strands of γ_* from
 666 the same pipe region cross, they define a trigon with a boundary of the region-intersection. By applying
 667 Corollary 3.2, we can make this trigon empty using monotonic homotopy moves, and then move the
 668 crossing outside of the intersection. This operation does not break Properties (1)–(4). Repeating this as
 669 many times as needed, γ_* satisfies Property (5) and thus respects the pipe system Π .

670 Then we claim that the closed walk $C_\Pi(\gamma_*)$ is identical to $C_\Pi(\gamma)$. Indeed, by Property (4), none
 671 of these closed walks contains spurs, and γ_* and γ are homotopic by definition. Since Π retracts (as
 672 a topological space) into its skeleton graph G , the claim follows from the fact that two closed walks
 673 without spurs in a graph are homotopic if and only if they are identical (up to cyclic permutation).

674 We straighten the tangle induced by γ_* within the cluster region using monotonic moves. Now, γ_*
 675 can be considered as a multicurve in the new pipe system $\tilde{\Pi}$, and furthermore, the closed walk $C_{\tilde{\Pi}}(\gamma_*)$
 676 induced by γ_* in $\tilde{\Pi}$ is identical to $C_{\tilde{\Pi}}(\tilde{\gamma})$. (Indeed, in general, for any curve $\alpha \subseteq \tilde{\Pi} \subseteq \Pi$, the closed walk
 677 $C_{\tilde{\Pi}}(\alpha)$ is simply obtained from $C_\Pi(\alpha)$ by replacing subwords wuv with subwords $w[wu][uv]v$. Because
 678 $C_\Pi(\gamma_*) = C_\Pi(\gamma)$ as shown above, one has $C_{\tilde{\Pi}}(\gamma_*) = C_{\tilde{\Pi}}(\tilde{\gamma})$.) From that we conclude that γ_* and $\tilde{\gamma}$
 679 are homotopic within $\tilde{\Pi}$.

680 Any curve in $\tilde{\Pi}$ that is tight in Π is also tight in $\tilde{\Pi}$. It follows that γ_* is tight within $\tilde{\Pi}$, and is therefore
 681 a tightening of $\tilde{\gamma}$ within $\tilde{\Pi}$. Thus it has exactly as many self-crossings as any tightening $\tilde{\gamma}_*$ of $\tilde{\gamma}$ within $\tilde{\Pi}$.
 682 This concludes the proof. \square

683 **Pipe expansion.** We perform the following *pipe expansion* on a pipe uv . For sake of analysis, we want
 684 to make sure that the pipe expansions we performed actually improve the quality of the multicurve
 685 in a pipe system. This motivates the following definitions [14, 19, 30]. Cluster u is a *base* of pipe uv
 686 if every vertex in $C(u)$ is incident to some edge in $C(uv)$. A pipe uv is *safe* if u and v are distinct and
 687 both u and v are bases of uv . A pipe uv in G is *useless* if both clusters incident to uv have degree 2 in G ;
 688 otherwise the pipe uv is *useful*. We will only perform pipe expansion on *safe* and *useful* pipes throughout
 689 the algorithm.

690 Let Δ be a topological ellipse containing the cluster regions D_u and D_v together with the pipe region
 691 R_{uv} , as well as portions of the pipe regions crossing R_{uv} (see Figure 4.3). By taking Δ close enough
 692 to the region R_{uv} , we can assume Δ contains no intersections between any two pipes intersecting R_{uv} .
 693 Because pipe uv is safe, the two cluster regions are distinct. We endow Δ with Euclidean metric such
 694 that all the ends are infinitesimally small, and position these ends so that there are no triple intersecting
 695 strands of D_u .

696 Then we modify γ by replacing every strand of Δ with a straight line. We modify G and Π accord-
 697 ingly, see Figure 4.3: For each pipe uw incident to u other than uv , create a new cluster $[uw]$, whose
 698 corresponding cluster region in Π is a neighborhood of the intersection between pipe region R_{uw} and
 699 the boundary of the disk Δ . Rename the pipe uw into $[uw]w$. Similarly for each pipe vw incident to v ,
 700 create a new cluster $[vw]$, whose corresponding cluster region in Π is a neighborhood of the end $A_{v,w}$,
 701 and rename the pipe vw into $[vw]w$. Because the pipe uv is safe, both u and v are bases of uv ; and G has
 702 no spurs as γ respects G . Therefore every strand of R_{uv} must connect an end of D_u to an end of D_v . For
 703 every pair of pipes uw and vw' , insert a pipe $[uw][vw']$ if there was a strand of Δ that connects end $A_{u,w}$
 704 with end $A_{v,w'}$; insert a corresponding rectangular pipe region in Π accordingly, so that in the drawing of
 705 G and Π the pipes intersect transversely. By the choice of Euclidean metric on Δ , these pipes can be
 706 taken to be arbitrarily thin rectangles such that no three of them overlap at a point. Finally, remove
 707 clusters u and v from G and regions D_u and D_v from Π .

708 **Lemma 4.4.** *First, the pipe expansion can be implemented using $O(n^2)$ monotonic homotopy moves,*
 709 *such that after the pipe expansion the new multicurve $\tilde{\gamma}$ still respects the modified pipe system $\tilde{\Pi}$. Second,*
 710 *if we denote by $\tilde{\gamma}_*$ a tightening of $\tilde{\gamma}$ within the modified pipe system $\tilde{\Pi}$ (viewed as a topological space),*
 711 *then $\tilde{\gamma}_*$ is also a tightening of γ within Π .*

712 The proof is virtually identical to the proof of Lemma 4.3; we repeat it here to be comprehensive.

713 **Proof:** Let uv be the useful pipe that we perform pipe expansion on. Topologically, this can be imple-
 714 mented by straightening the tangle inside the disk Δ using Lemma 3.1, which can be done in $O(n^2)$
 715 moves, as any crossing in the tangle is also a crossing of γ , which is upper bounded by n at any point of
 716 the algorithm because the homotopy process is monotone.

717 Next we prove that the modified multicurve $\tilde{\gamma}$ respects the modified pipe system $\tilde{\Pi}$, by showing
 718 Properties (1)–(5) (and thus also (6)). Properties (1)–(3) immediately follow from the new strands
 719 being straight lines and the disk being convex. As for Property (4), consider ends of two different types:
 720 ends of the form $A_{[uv],v}$ and ends of the form $A_{[uv],[vw']}$, where w and w' are clusters incident respectively
 721 to u and v in G . For ends of the first type, if γ intersects $A_{[uv],v}$ consecutively twice, the subpath of γ
 722 between the two intersections must lie inside D_u , and therefore must be a strand in D_u . This implies
 723 that γ did not respect Π as Property (4) was violated, a contradiction. For ends of the second type, as
 724 the new strands are all straight lines between the ends, and the cluster regions have been taken to be
 725 elliptical neighborhoods of the ends, each strand can cross the boundary of each cluster at most once.
 726 Property (5) follows from the fact that the pipe regions are infinitesimally thin, and thus generically
 727 there are no crossings within the intersection of two of those.

728 For the second item, let γ_* denote a tightening of γ within Π . We claim that γ_* can be made to respect
 729 the pipe system Π using monotonic homotopy moves (no matter how many). The proof follows closely
 730 the one of Lemma 4.2. As γ_* is tight, it contains no embedded monogons or bigons. We ensure that it
 731 does not form any bigon with any end of Π by undoing such bigons, starting from the innermost ones.
 732 As in that proof, γ_* now satisfies Properties (1)–(4), but it may fail to satisfy Property (5). Within the
 733 intersection of two pipe regions, if two strands of γ_* from the same pipe region cross, they define a trigon
 734 with a boundary of this intersection. By applying Corollary 3.2, we can make this trigon empty using
 735 monotonic homotopy moves, and then move the crossing outside of the intersection. This operation
 736 does not break Properties (1)–(4). Repeating this as many times as needed, γ_* satisfies Property (5) and
 737 thus respects the pipe system Π .

738 We claim that the closed walk $C_{\Pi}(\gamma_*)$ that it induces there is identical to $C_{\Pi}(\gamma)$. Indeed, by Property (4)
 739 of the pipe system, none of these closed walks contains spurs, and γ_* and γ are homotopic by definition.
 740 Since Π retracts (as a topological space) into its skeleton graph G , the claim follows from the fact that

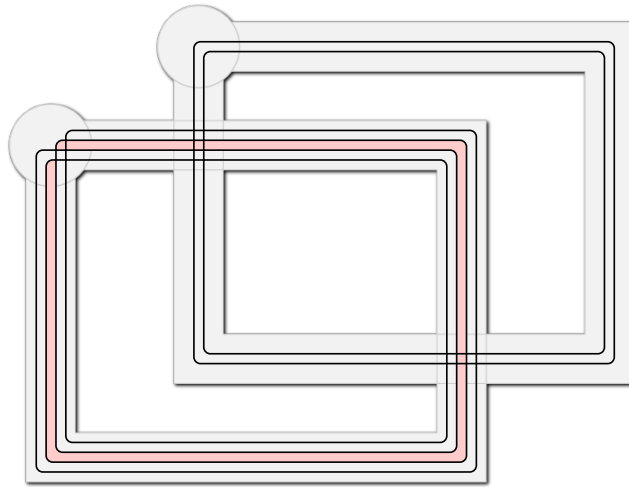


Figure 4.4. A multicurve γ in a canonical form on a sphere with four boundaries. Note that while the top-right curve is tightened, the bottom-left curve is not (an embedded bigon is labeled in pink).

741 two closed walks without spurs in a graph are homotopic if and only if they are identical (up to cyclic
742 permutation).

743 We straighten the tangles of γ_* within the cluster region using monotonic moves. Now, γ_* can be
744 considered as a curve of the new pipe system $\tilde{\Pi}$, and furthermore, the closed walk $C_{\tilde{\Pi}}(\gamma_*)$ induced by
745 γ_* in $\tilde{\Pi}$ is identical to $C_{\tilde{\Pi}}(\tilde{\gamma})$. (Indeed, in general, for any curve $\alpha \subseteq \tilde{\Pi} \subseteq \Pi$, the closed walk $C_{\tilde{\Pi}}(\alpha)$ is
746 simply obtained from $C_{\Pi}(\alpha)$ by replacing subwords $wuvw'$ with the subwords $w[wu][vw']w'$. Because
747 $C_{\Pi}(\gamma_*) = C_{\Pi}(\gamma)$ as shown above, this implies $C_{\tilde{\Pi}}(\gamma_*) = C_{\tilde{\Pi}}(\tilde{\gamma})$.) From that we conclude that γ_* and $\tilde{\gamma}$ are
748 homotopic within $\tilde{\Pi}$.

749 Any curve in $\tilde{\Pi}$ that is tight in Π is also tight in $\tilde{\Pi}$. It follows that γ_* is tight within $\tilde{\Pi}$, and is therefore
750 a tightening of $\tilde{\gamma}$ within $\tilde{\Pi}$. Thus it has exactly as many self-crossings as any tightening $\tilde{\gamma}_*$ of $\tilde{\gamma}$ within $\tilde{\Pi}$.
751 This concludes the proof. \square

752 4.3 Main algorithm

753 At the beginning of the algorithm, perform a cluster expansion on the unique cluster in the initial
754 pipe system Π_0 . Note that after this first expansion, the two incident clusters of any pipe are distinct.
755 The algorithm repeatedly performs pipe expansion on an arbitrary safe and useful pipe, until no such
756 pipe remains. Observe that after a cluster or pipe expansion, any newly created cluster is a base of
757 an incident pipe. Thus throughout the algorithm we maintain the invariant that every cluster is a
758 base of some pipe; in particular, this implies that there is always a safe pipe after the first cluster
759 expansion [19, Property 5] [14, §5.1] [30, Lemma 5].

760 **Lemma 4.5 (Chang et al. [14, Lemma 5.3], Fulek and Tóth [30, Lemma 5]).** *If every cluster in the*
761 *pipe system of G is a base of an incident pipe, but G has no useful pipes, then G must be a disjoint union*
762 *of cycles.*

763 By Lemma 4.5, when all the useful pipes are gone, the skeleton graph must be a disjoint union of
764 cycles. We now further put the multicurve into *canonical form*. A multicurve γ respecting a pipe system
765 Π is said to be in *canonical form* if (1) the skeleton graph G of Π is a disjoint union of cycles; (2)

766 every intersection of γ is either between two strands of different pipes, or lying in a unique cluster u^* ;
 767 furthermore, the strands in cluster u^* forms (the projection of) a braid. See Figure 4.4.

768 Let γ be a multicurve respecting a pipe system whose skeleton graph is a disjoint union of cycles.
 769 Slide all the crossings inside clusters to some arbitrarily chosen cluster u^* using multiple applications of
 770 Lemma 4.1, and perform Lemma 3.1 on u^* to straighten its strands [38, Propositions 14]; this can be
 771 done using $O(n^2)$ many monotonic homotopy moves. Now the multicurve must be in canonical form.
 772 De Graaf and Schrijver [38, Propositions 8 and 14] describe an algorithm to tighten any multicurve in
 773 canonical form using quadratically many monotonic homotopy moves. The main technical lemma [38,
 774 Proposition 7] can be described as a way to reduce the number of transpositions required to represent
 775 any permutation using conjugations. Intuitively, they show that as long as the multicurve is not tightened,
 776 for each constituent curve γ_i there is always a crossing that one can slide from the top of the braid all the
 777 way along the pipes where γ_i lies in, to the bottom of the braid and cancels out with another crossing
 778 using a $2 \rightarrow 0$ move, possibly after a sequence of $3 \rightarrow 3$ moves to adjust the position of the multicurve.

779 **Analysis.** Define the *potential function* $\Phi(C, G)$ to be the number of edges in C minus the number of
 780 pipes in G ; in notation, $\Phi(C, G) := |E(C)| - |E(G)| = \sum_{uv} (|C(uv)| - 1)$.

781 **Lemma 4.6 (Chang *et al.* [14, Lemma 5.4], Fulek and Tóth [30, Lemma 4]).** *Let γ be a multicurve*
 782 *respecting a pipe system Π , with corresponding closed walks C on skeleton graph G . Each pipe expansion*
 783 *performed on a useful pipe in Π decreases the potential $\Phi(C, G)$ by at least one.*

784 We now have all the tools to prove Lemma 1.5.

785 **Proof (of Lemma 1.5):** As the potential Φ is always nonnegative and the initial value is at most $O((g +$
 786 $b)n)$ by Lemma 4.2, the algorithm terminates after $O((g + b)n)$ steps by Lemma 4.6. Each cluster and
 787 pipe expansion can be implemented by $O(n^2)$ many homotopy moves (Lemmas 4.3 and 4.4). After
 788 no useful pipe remains, by Lemma 4.5 the skeleton graph must be a disjoint union of cycles. Turning
 789 γ into canonical form via Lemma 4.1, followed by tightening γ , using the algorithm by de Graaf and
 790 Schrijver [38], takes $O(n^2)$ many homotopy moves.

791 By Lemmas 4.3 and 4.4, a multicurve that is tight in the final pipe system is also tight in the original
 792 pipe system, which covers the entire surface. Therefore we have tightened the multicurve γ , and this
 793 proves Lemma 1.5. \square

794 5 Applications

795 5.1 Putting curves in minimal positions

796 In this subsection, we explain how our techniques can be leveraged to prove Theorem 1.2. Most of the
 797 steps of the proof are readily algorithmic, in particular the techniques of Section 4 have been designed
 798 with graph drawing applications in mind. While we have described many steps using geometry, this was
 799 just for convenience and the cluster and pipe expansion operations are purely combinatorial: instead
 800 of endowing the disks with a Euclidean metric, one can just choose an (arbitrary) arrangement of
 801 pseudolines describing how the infinitesimally thin pipe regions will cross.

802 In order to do the expansions, we rely on Lemma 3.1. While one could analyze the complexity of
 803 computing the right sequence of moves, let us just observe that for our application in mind—to compute
 804 a minimal position for the given multicurve—we can directly straighten the tangle within the disk. So
 805 the complexity of straightening a tangle with n crossings and m strands is simply $O(n + m)$. Each cluster

806 and pipe expansion can be realized in $O((g + b)n)$ time since there are $O((g + b)n)$ strands and $O(n)$
 807 crossings, therefore the time complexity of the steps described in Section 4 is $O((g + b)^2n^2)$.

808 The remaining algorithmic question is to carry out the straightening process described in Section 3,
 809 which relies heavily on hyperbolic geometry. Hyperbolic geometric computations are becoming increas-
 810 ingly common (see for example Jordanov and Teillaud [43]) in computational geometry, and the ones we
 811 rely on are no harder to carry out than the Euclidean ones. As is customary in computational geometry,
 812 we work in a real RAM model. For the sake of convenience, we allow computations of hyperbolic
 813 trigonometric functions and their inverses in constant time, but note that this is not strictly required as
 814 approximating those functions works equally well.

815 The first step of Section 3 is to endow the surface with a hyperbolic metric. In terms of algorithms,
 816 this is achieved by mapping the surface to a polygon in some model of hyperbolic geometry, for example
 817 the Poincaré disk. The vertices of the cut graph are mapped to the vertices of a regular hyperbolic
 818 polygon, and can thus be computed readily. The edges in the Poincaré disk model are portions of circles
 819 intersecting the boundary at right angles, and can therefore be encoded by their endpoints. Since the
 820 second step of the proof of Section 3 is to straighten the tangle of γ within this polygon, for an algorithm
 821 we can start directly with a straightened tangle, that is, a collection of circular arcs.

822 The main loop of the algorithm consists of taking a point of maximal tortuosity and straightening
 823 the tangle within a disk centered at this point. Since, throughout the tightening process, the curve γ
 824 stays a piecewise-geodesic, the points of maximal tortuosity are always at the vertices between two
 825 consecutive circular arcs. We loop on all these points to find the one with largest tortuosity. This requires
 826 length computations which can be done in constant time with inverse hyperbolic functions (note that
 827 approximating computations are also fine here, and thus adding such functions to the computation
 828 model is not strictly required).

829 We straighten the tangle in a disk centered at the point with maximum tortuosity, and each time
 830 such a straightening is done, the number of breaking points increases by one for each strand in the
 831 tangle. There is a potential pitfall here: each straightening could double the number of breaking
 832 points in the multicurve, which could lead to an exponential number of circular arcs. Furthermore, the
 833 number of intersections between the multicurve and the reduced cut graph might also increase during a
 834 straightening. However, we can prove that they do not increase too much.

835 **Lemma 5.1.** *Let Σ be endowed with the hyperbolic metric described in Section 3 for a cut graph X , and*
 836 *let γ be an n -vertex multicurve on Σ that crosses X at most $O(n)$ times such that all its segments between*
 837 *successive intersections with X are geodesics. After any number of straightenings of γ within a disk or*
 838 *within the polygon $\Sigma \setminus X$, the number of intersections of γ with X is $O(gn)$.*

839 **Proof:** When endowed with the hyperbolic metric described in Section 3, the edges of the cut graph
 840 are geodesic segments. We extend these segments into a family of $O(g)$ closed geodesics, which we
 841 denote by Δ . These extensions are closed because the hyperbolic metric has been obtained from an
 842 equilateral $O(g)$ -gon, and thus extending the geodesics just amounts to triangulating the polygon by
 843 adding a vertex at the center and connecting it to every vertex by geodesics. Since γ is geodesic within
 844 the polygon defined by X , it is made of $O(n)$ geodesic arcs, each of which crosses Δ at most $O(g)$ times,
 845 thus the number of intersections between γ and Δ is $O(gn)$. We claim that this number of intersections
 846 does not increase after any sequence of straightenings. Indeed, we can consider that each straightening
 847 is a straightening of $\gamma \cup \Delta$, viewed as a single multicurve. Since Δ is already made of geodesics, it is
 848 unchanged by the straightening. Since the straightening does not increase the number of crossings of
 849 the multicurve, the number of intersections of γ with Δ , and thus with X , is $O(gn)$. \square

850 Therefore, by inserting a straightening of all the strands within $\Sigma \setminus X$ between two straightenings

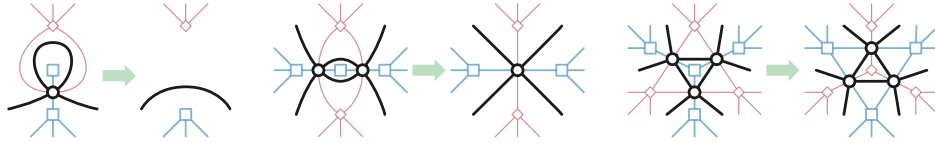


Figure 5.1. Electrical moves $1 \rightarrow 0$, $2 \rightarrow 1$, and $3 \rightarrow 3$.

851 within a disk, we can ensure that the multicurve γ is always made of $O(gn)$ geodesic segments, which
 852 we can encode using the coordinates of their endpoints.

853 The loop ends when no point of high tortuosity is found. It remains to find a point inside the
 854 hyperbolic polygon which is far away (under the hyperbolic metric) from a collection of polynomially
 855 many geodesic arcs. As we emphasized after the proof of Lemma 3.4, in hyperbolic geometry, the sets of
 856 points equidistant to a geodesic are called *hypercircles*, which are *not* geodesics (unlike in the Euclidean
 857 setting), but they are still realized by circular arcs in the Poincaré disk model. Therefore, one can easily
 858 compute all these hypercircles, and find a point to puncture in the complement of regions bounded by
 859 pairs of circles.

860 The bottleneck of the algorithm to move curves close to the geodesics is the sequence of straightenings
 861 in disks centered at points of high tortuosity: there are $O(n^3 \log^3 g/g^2)$ such straightenings. Each of them
 862 requires finding the correct breaking points among the $O(gn)$ possibilities, after which straightening the
 863 tangle also takes $O(gn)$ time. The resulting algorithm runs in $O(n^4 \log^3 g/g)$ time. In total, we can put
 864 a multicurve in minimal position in $O(n^4 \log^3 g/g + (g+b)^2 n^2)$ time.

865 **Handling the torus.** While our techniques do not apply to multicurves on a torus without boundary,
 866 this case can be handled manually using homology (see for example Stillwell [62, Chapter 5]). Indeed,
 867 the homotopy class of a closed curve on a torus coincides with its homology, which is a pair of integers
 868 $(p, q) \in \mathbb{Z}^2$. For a given multicurve γ , one can compute the corresponding collection of pairs of integers
 869 (p_i, q_i) in polynomial time by using any classical homology computation algorithm. Then a minimal
 870 position of the multicurve γ can be obtained by drawing γ on a Euclidean flat torus represented by a
 871 unit-square, where each closed curve is realized by a straight geodesic of slope q_i/p_i . If $\gcd(p_i, q_i) \neq 1$,
 872 we take $\gcd(p_i, q_i)$ many copies of the geodesic with a slight offset and connect them so as to realize
 873 the homology class (p, q) with exactly $\gcd(p_i, q_i) - 1$ self-crossings. This multicurve is homotopic to
 874 γ because it is homological to γ , and on the torus homology and homotopy coincide. It is in minimal
 875 position because any closed curve of homology (p, q) has at least $\gcd(p, q) - 1$ self-crossings, and the
 876 crossings between different components realize the *algebraic intersection number* $p_i q_j - p_j q_i$, of which
 877 the absolute value is known to lower bound the geometric intersection number.

878 5.2 Electrical reductions

879 Next, we consider the implication on reducing surface graphs using electrical transformations and sketch
 880 a proof of Theorem 1.3. As mentioned in the introduction, every k -terminal graph embedded on a
 881 surface Σ corresponds to a multicurve lying on a *punctured* surface through the medial construction by
 882 adding one puncture on Σ for each terminal in the graph. The set of facial electrical transformations
 883 corresponds to a set of local operations on multicurves called the *electrical moves*, which bear extreme
 884 similarity to the homotopy moves. Let $X(\gamma)$ denote the minimum number of electrical moves required to
 885 tighten γ on Σ , and let $H^\downarrow(\gamma)$ denote the minimum number of monotonic homotopy moves required
 886 to tighten γ on Σ , without ever increase the number of vertices. One can prove that if $H^\downarrow(\gamma) \leq f(n)$
 887 for any n -vertex multicurve on surface Σ , then $X(\gamma) \leq n \cdot f(n)$ holds, by replacing the first $2 \rightarrow 0$ move
 888 with a $2 \rightarrow 1$ move and recurse [10, Lemma 7.2]. In particular, our polynomial upper bound on the

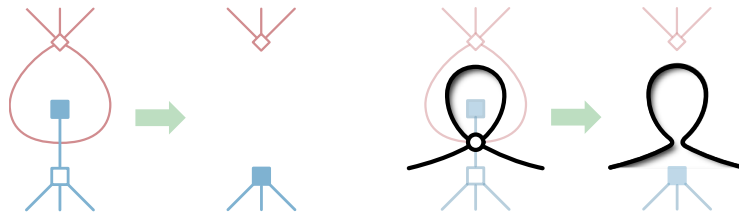


Figure 5.2. A terminal-leaf contraction on graph G and the corresponding operation on medial multicurve G^\times ; the blue solid squares represent the terminals in G , which turn into punctures on the surface.

889 number of monotonic homotopy moves directly implies a polynomial bound on the number of electrical
 890 moves required to tighten a multicurve. The original proof can be turned algorithmic by using the
 891 polynomial-time algorithm for monotonic homotopy from Theorem 1.2; we include a proof here to make
 892 the presentation complete.

893 **Lemma 5.2 (Chang [10, Lemma 7.2]).** *Fix an arbitrary surface Σ . Any polynomial running time $f(n)$*
 894 *for tightening any n -vertex multicurve γ on Σ using monotonic homotopy moves can be turned into a*
 895 *polynomial running time $n \cdot f(n)$ for tightening any n -vertex multicurve γ on Σ using electrical moves.*

896 **Proof:** Let γ be an arbitrary multicurve on Σ with n vertices. First, if multicurve γ is already tightened
 897 under homotopy moves, then it must be tight under electrical moves as well (see Chang, Cossarini, and
 898 Erickson [11, Lemma 3.7]) and thus the statement trivially holds. Otherwise, consider the first homotopy
 899 move in the algorithm for tightening γ monotonically (from Theorem 1.2) that decreases the number
 900 of vertices in γ (that is, either a $1 \rightarrow 0$ or $2 \rightarrow 0$ move). Replace the $2 \rightarrow 0$ move with a $2 \rightarrow 1$ if needed, one
 901 arrives at a curve γ' that has strictly fewer vertices than γ . We restart the monotonic homotopy algorithm
 902 on γ' instead.

903 The time spent from reducing γ to γ' is at most $f(n)$. Now by induction on the number of vertices,
 904 the time $g(n)$ for reducing γ is

$$\begin{aligned}
 905 \quad g(n) &\leq g(n-1) + f(n) \\
 906 &\leq (n-1) \cdot f(n-1) + f(n) \\
 907 &\leq n \cdot f(n), \\
 908
 \end{aligned}$$

909 which proves the lemma. □

910 5.3 Terminal-leaf contraction

911 Previous works [7, 21, 29, 34] on reducing surface graphs with terminals using electrical transformations
 912 also rely on an additional move which is not a facial electrical move. The **terminal-leaf contraction**⁶ is a
 913 leaf-reduction performed on a terminal by contracting its unique incident edge and assigning the merged
 914 vertex as a new terminal. See Figure 5.2 for a graph- and curve-view of this operation. First thing to
 915 notice is that a multicurve that is tight under electrical moves might not be tight when terminal-leaf
 916 contractions are allowed. We will argue that after the multicurve is tightened using electrical moves,
 917 we can further reduce the curve efficiently using terminal-leaf contractions, until nothing can be done.
 918 This yields the desired polynomial bounds on number of monotonic homotopy moves, as well as a
 919 polynomial-time algorithm. To this end we first introduce the following concepts.

⁶also known as the *FP-assignment* [33], after Feo and Provan [29]

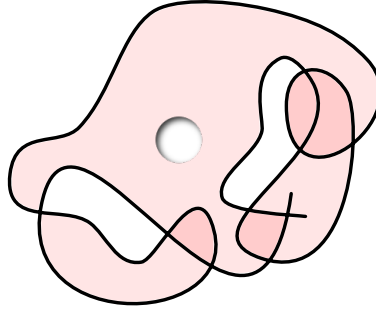


Figure 5.3. A punctured monogon α and the image of its singular disk.

920 **Punctured monogon.** A *smoothing* of a multicurve γ at a vertex x replaces the intersection of γ
 921 around x with two disjoint simple paths, so that the result is another multicurve; notice that there are
 922 two possible smoothings at each vertex. More generally, a *smoothing* of a multicurve γ is any multicurve
 923 obtained by smoothing a subset of its vertices. A multicurve γ contains a (singular) **punctured monogon**
 924 α if γ has a constituent curve γ_i with a crossing x such that after smoothing γ_i at x in the way that
 925 disconnects γ_i , one of the two curves of the smoothing is freely homotopic to a small circle going exactly
 926 once around a single puncture of Σ . We call x the **tip** of punctured monogon α . This small circle bounds
 927 an embedded punctured disk, which turns into a singular punctured disk under the homotopy. (This is
 928 akin to diagrams used in geometric and combinatorial group theory, see e.g. [48].) The monogon α itself
 929 designates this singular disk, that is, a map $\alpha: D^2 \rightarrow \Sigma$ such that $\alpha(D^2)$ covers the puncture exactly once.
 930 See Figure 5.3 for an example. A punctured monogon α is **empty** if $\alpha(\partial D_2)$ is simple and the interior
 931 of $\alpha(D^2)$ is disjoint from γ . A (medial) terminal-leaf contraction always applies on empty punctured
 932 monogons. By definition punctured monogons are exactly those objects that are homotopic to some
 933 empty punctured monogon.

934 As a sanity check to see that punctured monogons are the right objects to work with, observe that
 935 any tight multicurve on a sphere with three punctures can be made simple by removing all the punctured
 936 monogons; this corresponds exactly to the statement that any 3-terminal plane graph can be reduced
 937 completely using electrical transformations along with terminal-leaf contractions [33].

938 First, we show that any punctured monogon can be removed efficiently.

939 **Lemma 5.3.** *Let γ be a multicurve with n crossings in minimal position on a surface Σ . If γ contains a*
 940 *punctured monogon, then we can compute in $O(n^3)$ time a sequence of $O(n^3)$ 3→3 moves transforming*
 941 *γ into a multicurve γ' containing an empty punctured monogon.*

942 **Proof:** Let α be a punctured monogon in γ . Our plan for the proof is to first turn α into an embedded
 943 disk (with a puncture), then empty it. Smooth the vertex x in γ (by removing a small neighborhood of
 944 x in γ and reconnecting the curves in a non-crossing fashion) so that the punctured monogon α turns
 945 into a closed curve, which we denote as $\check{\alpha}$. By definition of punctured monogon, $\check{\alpha}$ is homotopic to a
 946 simple curve winding around the puncture. A result of Hass and Scott [40, Theorem 2.4] shows that if
 947 $\check{\alpha}$ is not simple, there must be an embedded bigon or monogon in $\check{\alpha}$ that contains x on the boundary
 948 (because γ itself is in minimal position). Therefore such a bigon (resp. monogon) corresponds to a trigon
 949 (resp. bigon) in γ . By minimality of γ , the only possibility is that this is a trigon. Using Lemma 2.2 and
 950 Corollary 3.2 we can empty and flip the trigon in γ (and thus the bigon in $\check{\alpha}$) using at most $O(n^2)$ moves.
 951 Now the complexity of $\check{\alpha}$ decreases; after at most n steps we turn $\check{\alpha}$ into a simple closed curve. We
 952 emphasize that as γ is already tight, and the complexity of γ does not change throughout the process.

953 At this stage, the singular disk of α is embedded. If we consider the surface Σ without the puncture,
 954 α forms an embedded monogon. Let α' be an innermost embedded monogon inside α (possibly $\alpha = \alpha'$).

955 Considering Σ again with the puncture, since γ is in minimal position, α' must be a punctured monogon.
 956 Since it is innermost, all the strands crossing α' are simple. Any such strand bounds a trigon with the
 957 tip of α' , which we can remove once again using Corollary 3.2. This does not increase the number
 958 of crossing strands with the α' . Thus, removing all such strands costs $O(n^3)$ moves, after which the
 959 punctured monogon α' is empty. \square

960 **Routing set.** Next we show that when there are no more punctured monogons, the multicurve must
 961 be tight under electrical moves and terminal-leaf contractions.

962 For any multicurve γ , the **routing set** [11] of γ is the following collection of homotopy classes:

$$963 \quad \mathit{route}(\gamma) := \{ [\check{\gamma}] \mid \check{\gamma} \text{ is a smoothing of } \gamma \}.$$

964 Each homotopy class in $\mathit{route}(\gamma)$ is referred to as a **route** of γ . A key property is that the routing set is
 965 invariant under electrical moves [11, Lemma 3.6].

966 **Lemma 5.4.** *Let γ be a connected multicurve in minimal position on a surface Σ . If γ does not contain a*
 967 *punctured monogon, then no sequence of electrical moves and terminal-leaf contractions can transform γ*
 968 *into another multicurve with fewer crossings than γ .*

969 **Proof:** Assume otherwise that there is a sequence of electrical moves and terminal-leaf contractions
 970 transforming γ into another multicurve with fewer crossings. Let the number of terminal-leaf contractions
 971 used in this sequence be minimal among all counterexamples. If no terminal-leaf contraction is used,
 972 then the fact that γ is tight under electrical moves is a theorem of Chang, Cossarini and Erickson [11,
 973 Lemma 3.7].

974 Otherwise, denote by γ' and γ'' the two multicurves just before and after the first terminal-leaf
 975 contraction is used. The curve γ' contains an empty punctured monogon, whose tip is denoted by x . We
 976 emphasize that γ' might not be in minimal position. We first claim that γ is homotopic to a smoothing
 977 of γ'' . By definition, γ' is related to γ by electrical moves, thus $\mathit{route}(\gamma') = \mathit{route}(\gamma)$. Therefore γ is
 978 homotopic to a smoothing $\check{\gamma}'$ of γ' . A theorem of Neumann-Coto⁷ [50, Proposition 2.2] shows that
 979 a tightening of $\check{\gamma}'$ can be found among the smoothings of $\check{\gamma}'$, and thus of γ' . Therefore without loss
 980 of generality we can take $\check{\gamma}'$ to be in minimal position. Assume for contradiction that x has not been
 981 smoothed in $\check{\gamma}'$. Denote by κ' the constituent curve of $\check{\gamma}'$ containing x , and κ the constituent curve of γ
 982 homotopic to κ' . Since κ and κ' are homotopic and both in minimal position, they can be transformed
 983 into each other via only 3→3 moves (see for example Hass and Scott [41, Theorem 2.1]). Since 3→3
 984 moves preserve punctured monogons and γ (and thus κ) has no punctured monogon, we have that
 985 κ' contains no punctured monogon, a contradiction. So the vertex x has been smoothed in $\check{\gamma}'$. While
 986 there are two possible ways to smooth x , one of them disconnects the multicurve which is impossible
 987 because γ is a connected multicurve in minimal position and also homotopic to $\check{\gamma}'$. The other smoothing,
 988 if performed on γ' , gives us γ'' ; this implies that $\check{\gamma}'$ can be viewed as a smoothing of γ'' . Therefore, γ is
 989 homotopic to a smoothing of γ'' .

990 Since γ' and γ are related via electrical moves, by Chang, Cossarini and Erickson [11, Lemma 3.1], γ''
 991 (which is a smoothing of γ') is related via electrical moves to a smoothing $\check{\gamma}$ of γ . If $\check{\gamma} = \gamma$, then doing the
 992 moves in reverse, we have removed the need of a terminal-leaf contraction between γ and γ'' and thus
 993 this contradicts the minimality of the number of terminal-leaf contractions used in our counter-example.
 994 Otherwise, γ is homotopic to a smoothing of γ'' , thus is in $\mathit{route}(\gamma'')$, and thus in $\mathit{route}(\check{\gamma})$. Thus γ is
 995 homotopic to one of its strict smoothings, which contradicts that γ is in minimal position. \square

⁷Neumann-Coto's proposition requires the multicurve to be made of primitive curves. But in the proof, this is actually only needed to apply a theorem of Hass and Scott on monotonic simplification of curves, which is valid also for non-primitive multicurves, as was proved by de Graaf and Schrijver [38] (or our Lemma 1.5).

996 Now we are ready to prove the main result that any multicurve can be tightened using electrical
 997 moves and terminal-leaf contractions in polynomial time.

998 **Theorem 5.5.** *Any multicurve γ on a surface Σ with n vertices can be tightened using electrical moves
 999 and terminal-leaf contractions in $((g + b) \cdot n^5)$ time.*

1000 **Proof:** Let γ be an arbitrary multicurve on Σ with n vertices. Our recursive algorithm loops as follows.

1001 By Lemma 1.5 and Lemma 5.2, one can tighten γ into another multicurve γ' using electrical moves
 1002 in $O((g + b) \cdot n^4)$ time. Now γ' is in minimal position. Without loss of generality, γ' is connected, as
 1003 disconnected components cannot interact with each other under electrical moves and terminal-leaf
 1004 contractions. For each vertex x of γ' we test whether x is the tip of a punctured monogon using a
 1005 linear-time homotopy test [26, 46]. If γ' contains no punctured monogon, by Lemma 5.4, γ' is tight under
 1006 electrical moves and terminal-leaf contractions. Otherwise, if γ' contains a punctured monogon, by
 1007 Lemma 5.3, we can compute in $O(n^3)$ time a sequence of $O(n^3)$ 3→3 moves turning γ' into a multicurve
 1008 containing an empty punctured monogon. Applying a terminal-leaf contraction on this empty punctured
 1009 monogon, we obtain a new multicurve γ'' with $n - 1$ vertices, and we go back to the start of the loop.

1010 Since the number of vertices strictly decreases, the bottleneck of the algorithm is to tighten γ using
 1011 electrical moves and applying Lemma 5.3. The total running time is $O((g + b) \cdot n^5)$. \square

1012 **Acknowledgments.** The authors would like thank Jeff Erickson and Francis Lazarus for helpful discus-
 1013 sions, and Gelasio Salazar for his comments on earlier version of the paper.

1014 References

- 1015 [1] Sheldon B. Akers, Jr. The use of wye-delta transformations in network simplification. *Oper. Res.*
 1016 8(3):311–323, 1960.
- 1017 [2] Hugo A. Akitaya, Greg Aloupis, Jeff Erickson, and Csaba D. Tóth. Recognizing weakly simple
 1018 polygons. *Discrete & Computational Geometry* 58(4):785–821, 2017.
- 1019 [3] Hugo A. Akitaya, Radoslav Fulek, and Csaba D. Tóth. Recognizing weak embeddings of graphs.
 1020 *Proceedings of the Twenty-Ninth Annual ACM-SIAM Symposium on Discrete Algorithms*, 274–292,
 1021 2018.
- 1022 [4] James W. Alexander. Combinatorial analysis situs. *Trans. Amer. Math. Soc.* 28(2):301–326, 1926.
- 1023 [5] James W. Alexander and G. B. Briggs. On types of knotted curves. *Ann. Math.* 28(1/4):562–586,
 1024 1926–1927.
- 1025 [6] Sigurd Angenent. Parabolic equations for curves on surfaces: Part II. Intersections, blow-up and
 1026 generalized solutions. *Ann. Math.* 133(1):171–215, 1991.
- 1027 [7] Dan Archdeacon, Charles J. Colbourn, Isidoro Gitler, and J. Scott Provan. Four-terminal reducibility
 1028 and projective-planar wye-delta-wye-reducible graphs. *J. Graph Theory* 33(2):83–93, 2000.
- 1029 [8] Ara Basmajian, Hugo Parlier, and Juan Souto. Geometric filling curves on surfaces. *Bulletin of the*
 1030 *London Mathematical Society* 49(4):660–669. Wiley Online Library, 2017.
- 1031 [9] Edward A. Bender and E. Rodney Canfield. The asymptotic number of rooted maps on a surface. *J.*
 1032 *Comb. Theory Ser. A* 43:244–257, 1986.

- 1033 [10] Hsien-Chih Chang. *Tightening curves and graphs on surfaces*. Ph.D. dissertation, University of Illinois
1034 at Urbana-Champaign, 2018.
- 1035 [11] Hsien-Chih Chang, Marcos Cossarini, and Jeff Erickson. Lower bounds for electrical reduction on
1036 surfaces. *35th International Symposium on Computational Geometry (SoCG 2019)*, 25:1–25:16, 2019.
1037 Leibniz International Proceedings in Informatics (LIPIcs) 129, Schloss Dagstuhl–Leibniz-Zentrum
1038 fuer Informatik. (<http://drops.dagstuhl.de/opus/volltexte/2019/10429>).
- 1039 [12] Hsien-Chih Chang and Jeff Erickson. Untangling planar curves. *Discrete & Computational Geometry*
1040 58(4):889–920, 2017.
- 1041 [13] Hsien-Chih Chang, Jeff Erickson, Arnaud de Mesmay, David Letscher, Saul Schleimer, Eric Sedgwick,
1042 Dylan Thurston, and Stephan Tillmann. Untangling curves on surfaces via local moves. *Proc. 29th*
1043 *Annual ACM-SIAM Symposium on Discrete Algorithms*, 121–135, 2018.
- 1044 [14] Hsien-Chih Chang, Jeff Erickson, and Chao Xu. Detecting weakly simple polygons. Preprint, 2014.
1045 arXiv:1407.3340.
- 1046 [15] Hsien-Chih Chang, Jeff Erickson, and Chao Xu. Detecting weakly simple polygons. *Proc. 26th*
1047 *ACM-SIAM Symp. Discrete Algorithms*, 1655–1670, 2015.
- 1048 [16] Charles J. Colbourn, J. Scott Provan, and Dirk Vertigan. A new approach to solving three combina-
1049 torial enumeration problems on planar graphs. *Discrete Appl. Math.* 60:119–129, 1995.
- 1050 [17] Éric Colin de Verdière and Jeff Erickson. Tightening non-simple paths and cycles on surfaces. *SIAM*
1051 *J. Comput.* 39(8):3784–3813, 2010.
- 1052 [18] Yves Colin de Verdière, Isidoro Gitler, and Dirk Vertigan. Réseaux électriques planaires II. *Comment.*
1053 *Math. Helvetici* 71:144–167, 1996.
- 1054 [19] Pier Francesco Cortese, Giuseppe Di Battista, Maurizio Patrignani, and Maurizio Pizzonia. On
1055 embedding a cycle in a plane graph. *Discrete Mathematics* 309(7):1856–1869, 2009.
- 1056 [20] Max Dehn. Über unendliche diskontinuierliche Gruppen. *Math. Ann.* 71(1):116–144, 1911.
- 1057 [21] Lino Demasi and Bojan Mohar. Four terminal planar Delta-Wye reducibility via rooted $K_{2,4}$ minors.
1058 *Proc. 26th Ann. ACM-SIAM Symp. Discrete Algorithms*, 1728–1742, 2015.
- 1059 [22] Vincent Despré and Francis Lazarus. Computing the geometric intersection number of curves. *33rd*
1060 *International Symposium on Computational Geometry (SoCG 2017)*, 2017.
- 1061 [23] David Eppstein. Dynamic generators of topologically embedded graphs. *Proc. 14th Ann. ACM-SIAM*
1062 *Symp. Discrete Algorithms*, 599–608, 2003. arXiv:cs.DS/0207082.
- 1063 [24] Jeff Erickson and Sarel Har-Peled. Optimally cutting a surface into a disk. *Discrete Comput. Geom.*
1064 31(1):37–59, 2004.
- 1065 [25] Jeff Erickson and Amir Nayyeri. Minimum cuts and shortest non-separating cycles via homology
1066 covers. *Proc. 22nd Ann. ACM-SIAM Symp. Discrete Algorithms*, 1166–1176, 2011.
- 1067 [26] Jeff Erickson and Kim Whittlesey. Transforming curves on surfaces redux. *Proc. 24th Ann. ACM-SIAM*
1068 *Symp. Discrete Algorithms*, 1646–1655, 2013.

- 1069 [27] Benson Farb and Dan Margalit. *A Primer on Mapping Class Groups*. Princeton Math. Series 50.
1070 Princeton Univ. Press, 2011. (<http://www.math.utah.edu/~margalit/primer/>).
- 1071 [28] Thomas A. Feo. *I. A Lagrangian Relaxation Method for Testing The Infeasibility of Certain VLSI Routing*
1072 *Problems. II. Efficient Reduction of Planar Networks For Solving Certain Combinatorial Problems*.
1073 Ph.D. thesis, Univ. California Berkeley, 1985. (<http://search.proquest.com/docview/303364161>).
- 1074 [29] Thomas A. Feo and J. Scott Provan. Delta-wye transformations and the efficient reduction of
1075 two-terminal planar graphs. *Oper. Res.* 41(3):572–582, 1993.
- 1076 [30] Radoslav Fulek and Csaba D. Tóth. Crossing minimization in perturbed drawings. *GD 2018: Graph*
1077 *Drawing and Network Visualization*, 229–241, 2018.
- 1078 [31] Radoslav Fulek and Csaba D. Tóth. Atomic embeddability, clustered planarity, and thickenability.
1079 Manuscript, Dec 2019. arXiv:1907.13086.
- 1080 [32] Meinolf Geck and Gotz Pfeiffer. On the irreducible characters of Hecke algebras. *Advances in*
1081 *Mathematics* 102(1):79–94, 1993.
- 1082 [33] Isidoro Gitler. *Delta-wye-delta Transformations: Algorithms and Applications*. Ph.D. dissertation,
1083 Department of Combinatorics and Optimization, University of Waterloo, 1991.
- 1084 [34] Isidoro Gitler and Feliú Sagols. On terminal delta-wye reducibility of planar graphs. *Networks*
1085 57(2):174–186, 2011.
- 1086 [35] Jay R. Goldman and Louis H. Kauffman. Knots, tangles, and electrical networks. *Adv. Appl. Math.*
1087 14:267–306, 1993.
- 1088 [36] Jacob E. Goodman and Stefan Felsner. Pseudoline arrangements. *Handbook of discrete and*
1089 *computational geometry*, 3rd edition, chapter 5, 125–157, 2017. Chapman and Hall/CRC.
- 1090 [37] Gramoz Goranci, Monika Henzinger, and Pan Peng. Improved guarantees for vertex sparsification
1091 in planar graphs. Preprint, December 2017. arXiv:1702.01136.
- 1092 [38] Maurits de Graaf and Alexander Schrijver. Making curves minimally crossing by Reidemeister
1093 moves. *J. Comb. Theory Ser. B* 70(1):134–156, 1997.
- 1094 [39] Matthew A. Grayson. Shortening embedded curves. *Ann. Math.* 129(1):71–111, 1989.
- 1095 [40] Joel Hass and Peter Scott. Intersections of curves on surfaces. *Israel J. Math.* 51:90–120, 1985.
- 1096 [41] Joel Hass and Peter Scott. Shortening curves on surfaces. *Topology* 33(1):25–43, 1994.
- 1097 [42] Joel Hass and Peter Scott. Configurations of curves and geodesics on surfaces. *Proceedings of the*
1098 *Kirbyfest*, 201–213, 1999. Geometry & Topology Monographs 2, Mathematical Sciences Publishers.
- 1099 [43] Jordan Iordanov and Monique Teillaud. Implementing Delaunay Triangulations of the Bolza
1100 Surface. *33rd International Symposium on Computational Geometry (SoCG 2017)*, 44:1–44:15,
1101 2017. Leibniz International Proceedings in Informatics (LIPIcs) 77, Schloss Dagstuhl–Leibniz-
1102 Zentrum fuer Informatik. (<http://drops.dagstuhl.de/opus/volltexte/2017/7217>).
- 1103 [44] François Jaeger. On spin models, triply regular association schemes, and duality. *J. Alg. Comb.*
1104 4:103–144, 1995.

- 1105 [45] Arthur Edwin Kennelly. Equivalence of triangles and three-pointed stars in conducting networks.
1106 *Electrical World and Engineer* 34(12):413–414, 1899.
- 1107 [46] Francis Lazarus and Julien Rivaud. On the homotopy test on surfaces. *2012 IEEE 53rd Annual*
1108 *Symposium on Foundations of Computer Science*, 440–449, 2012.
- 1109 [47] Alfred Lehman. Wye-delta transformations in probabilistic network. *J. Soc. Indust. Appl. Math.*
1110 11:773–805, 1963.
- 1111 [48] Roger C. Lyndon and Paul E. Schupp. *Combinatorial Group Theory*. Classics in Mathematics.
1112 Springer-Verlag, 2001.
- 1113 [49] Hiroyuki Nakahara and Hiromitsu Takahashi. An algorithm for the solution of a linear system
1114 by Δ -Y transformations. *IEICE TRANSACTIONS on Fundamentals of Electronics, Communications*
1115 *and Computer Sciences* E79-A(7):1079–1088, 1996. Special Section on Multi-dimensional Mobile
1116 Information Network.
- 1117 [50] Max Neumann-Coto. A characterization of shortest geodesics on surfaces. *Algebraic & Geometric*
1118 *Topology* 1:349–368, 2001.
- 1119 [51] Steven D. Noble and Dominic J. A. Welsh. Knot graphs. *J. Graph Theory* 34(1):100–111, 2000.
- 1120 [52] Sofya Poger. *Some New Results on Three-Terminal Planar Graph Reducibility*. Ph.D. dissertation,
1121 Stevens Inst. Tech., 2001.
- 1122 [53] Igor Prlina, Marcus Spradlin, and Stefan Stanojevic. All-loop singularities of scattering amplitudes
1123 in massless planar theories. Preprint, May 2018. arXiv:[1805.11617](https://arxiv.org/abs/1805.11617).
- 1124 [54] Kurt Reidemeister. *Knotentheorie*. Ergebnisse der Mathematik und ihrer Grenzgebiete 1. Springer,
1125 1932.
- 1126 [55] Gerhard Ringel. Teilungen der Ebene durch Geraden oder topologische Geraden. *Math. Z.* 64(1):79–
1127 102, 1956.
- 1128 [56] Gerhard Ringel. Über geraden in allgemeiner lage. *Elemente der Mathematik* 12:75–82, 1957.
- 1129 [57] Alexander Schrijver. On the uniqueness of kernels. *J. Comb. Theory Ser. B* 55:146–160, 1992.
- 1130 [58] Marc Shepard. *The topology of shortest curves in surfaces*. Ph.D. thesis, University of California,
1131 Berkeley, 1991.
- 1132 [59] Ernesto Staffelli and Federico Thomas. Analytic formulation of the kinestatis of robot manipulators
1133 with arbitrary topology. *Proc. 2002 IEEE Conf. Robotics and Automation*, 2848–2855, 2002.
- 1134 [60] Ernst Steinitz. Polyeder und Raumeinteilungen. *Enzyklopädie der mathematischen Wissenschaften*
1135 *mit Einschluss ihrer Anwendungen* III.AB(12):1–139, 1916.
- 1136 [61] Ernst Steinitz and Hans Rademacher. *Vorlesungen über die Theorie der Polyeder: unter Einschluß*
1137 *der Elemente der Topologie*. Grundlehren der mathematischen Wissenschaften 41. Springer-Verlag,
1138 1934. Reprinted 1976.
- 1139 [62] John Stillwell. *Classical Topology and Combinatorial Group Theory*, 2nd edition. Graduate Texts in
1140 Mathematics 72. Springer-Verlag, 1993.

- 1141 [63] Peter Guthrie Tait. On knots I. *Proc. Royal Soc. Edinburgh* 28(1):145–190, 1876–7.
- 1142 [64] Tiffani Traver. Trigonometry in the hyperbolic plane. Manuscript, May 2014.
- 1143 [65] Klaus Truemper. On the delta-wye reduction for planar graphs. *J. Graph Theory* 13(2):141–148,
1144 1989.
- 1145 [66] Takeshi Yajima and Shin’ichi Kinoshita. On the graphs of knots. *Osaka Mathematical Journal*
1146 9(2):155–163. Department of Mathematics, Osaka University, 1957.
- 1147 [67] Ron Zohar and Dan Gieger. Estimation of flows in flow networks. *Europ. J. Oper. Res.* 176:691–706,
1148 2007.